Simulation of extreme rainfall and streamflow events in small Mediterranean watersheds with a one-way coupled atmospheric-hydrologic modelling system

Corrado Camera[1], Adriana Bruggeman[2], George Zittis[3], Ioannis Sofokleous[2], and Joël Arnault[4]

[1] Dipartimento di Scienze della Terra 'A. Desio', Università degli Studi di Milano, Milano, 20133, Italy
[2] Energy Environment and Water Research Center, The Cyprus Institute, Nicosia, 2121, Cyprus
[3] Climate and Atmosphere Research Center, The Cyprus Institute, Nicosia, 2121, Cyprus
[4] Institute of Meteorology and Climate Research, Karlsruhe Institute of Technology, Garmisch-Partenkirchen, 82467, Germany

Correspondence to: Corrado Camera (corrado.camera@unimi.it)

Answers to reviewers

We would like to thank both reviewers for the time they took in commenting our manuscript. We found their comments very useful to improve our study. We incorporate most of them in the new version of the manuscript. Details regarding the work we have done on it can be found in the following answers.

Anonymous Referee # 1

The paper of Camera et al. presents a complete hydrometeorological reanalysis of two high impact events in Cyprus island (Eastern Mediterranean) addressing the challenge of effective reconstruction of such kind of events for small to very small catchments (ranging from 5 to less than 100 km^2 in this study). Overall, the paper presents a detailed and complete exercise, which adds another piece to the puzzle, benefiting from the availability of increasingly advanced modelling systems at all scales of analysis. Furthermore, the analysis is performed over an extraordinarily important area for Cyprus water resources, using a considerable set of discharge data and also (even though partially) with the challenging issue of hydrological modelling in a mountain environment with rock fractures. I suggest three main improvements to the paper, listed below, and have some other minor comments. I hope my comments are helpful to further enhance the quality of the paper.

1. My first main comment concerns the GCM data source (i.e., ERA-Interim). I acknowledge that this study inherits the work done by Zittis et al. (2017), but this global reanalysis is now replaced by the ERA5 reanalysis. This point is important, also given the fact that ERA5 offers ensemble members, which could be very usefully used exactly for the problem analysed (i.e., hydrometeorological chains targeted to small and very small catchments). I ask the authors to deal with this point, of course not requiring new simulations with ERA5, but discussing it.

   The decision to use ERA-Interim was driven by the previous work of Zittis et al. (2017) and also by the fact that we wanted to downscale a re-analysis dataset that was closer to the resolution of existing forecasting, decadal prediction, and global climate models in order to resemble a realistic modelling chain for forecasting applications. Moreover, ERA5 is not yet in a very mature stage, as evidenced from the emails alerting users from time to time to the presence of errors in the database. Also, in some cases re-runs are released for some years because of simulation errors (Simmons et al., 2020). However, we agree that ERA5 represents an opportunity for future improvement of the model skills. We have added few lines in the abstract and a discussion of the matter in Section 5.3.

   Abstract, Line 18-19: "This set up resembles a realistic modelling chain for forecasting applications and climate projections".

   Results, section 5.3 WRF-Hydro simulations with modeled precipitation, Line 481-486: "The rainfall fields modelled by Zittis et al. (2017) and used in this study were downscaled from the ERA-Interim re-analysis dataset. The decision to use these modelled data was driven by the fact that ERA-Interim presents a resolution closer to that of existing forecasting, decadal prediction, and global climate models, therefore it resembles a modelling chain for forecasting

applications and climate change projections (e.g., Reyers et al., 2019; Saha et al., 2014). For future studies ERA5, thanks to its finer resolution and the availability of ensemble members for uncertainty estimates, will be a valuable data source for improving the modelling chain over small (< 100 km^2) catchments".

2. Furthermore, I have some concerns about the calibration and use of the bucket model. In general, my idea is that the baseflow bucket model could not be so important for such short-time events. Indeed, the case studies analysed are rather impulsive. Furthermore, I think that the effects of the bucket model are somehow misinterpreted (please refer to a specific comment below). I suggest the authors revise and comment on their choice of calibrating in detail the baseflow bucket model.
   The hydrograph recession is made up of delayed surface runoff, interflow (lateral subsurface flow from the soil) and baseflow (groundwater). As suggested by Reviewer 1 in specific comment 20, we investigated the possibility to fit it by calibrating the overland roughness routing factor (OVRGH). We tested the sensitivity of OVRGH and we noticed that the parameter wasn't helpful in redistributing discharge, it was just increasing or decreasing it without modifying the shape of the hydrograph (new Fig. 3 and Fig. 4). In addition, for our runs we had already set OVRGH=1, which according to many authors is the maximum possible value that can be assigned to the parameter (Yucel et al., 2015; Verri et al., 2017). Therefore, we tried to capture the hydrograph recession better by increasing baseflow through the calibration of the reservoir (bucket) maximum volume (Z_{max}) and exponent (α). For Z_{max}, we aimed to set its value so that the reservoir could be filled between 10 January at h. 00:00 and 11 January at h. 12:00, indicatively within few hours and 2 days after the peak rainfall. The model redistributes the deep percolation exceeding the reservoir volume between the channel cells of the corresponding watersheds. For those watersheds that highly overestimated the baseflow due to spilling out of the groundwater reservoir, we further increased Z_{max}. For the exponent, we calibrated it fitting the pre-peak hydrograph. Details regarding how we modified the manuscript to incorporate these analyses and their results are given in the answers to the specific comments.

3. Finally, I believe the authors can go more into details analysing the catchments with rock fractures, which show too low performances that should be increased somehow (please refer to specific comments below).
   We tackled the problem from two sides. First, we modified the terrain slope categories (SLOPECAT) map and consequently the SLOPE coefficients (controlling deep drainage) based on geology. For gabbro and ultramafic rock types we forced a SLOPECAT resulting in a SLOPE coefficient equal to 1 (i.e., the maximum possible value) and therefore in a maximization of the drainage from the soil column to the groundwater reservoir. Second, based on geology and field observations (Camera et al., 2018), we modified the soil type map as well. The MODIS database, which was used for soil characterization, attributes a uniform clay loam soil texture to the Troodos Mountains. However, we have observed that at the higher elevations, where predominant geology is gabbro and ultramafic rocks, soils show a gravelly sandy loam texture

(Camera et al., 2018). Therefore, we modified the MODIS map, attributing a sandy loam soil type for cells characterized by gabbro and ultramafic rocks. In the WRF-Hydro model, soil properties are linked to soil type. For the cell involved, this change of soil type resulted in a modification (among other properties) of the saturated hydraulic conductivity from 2.45E-6 m/s to 5.32E-6 m/s. Before applying these changes, we investigated the sensitivity of the saturated hydraulic conductivity (Ks), which was found to be a sensitive parameter (see new Fig. 3).
Despite our efforts to maximize infiltration and deep drainage to reduce the hydrograph peak, the model still overestimated the observed flow in the high elevation watersheds. Looking at observed temperature time series, it is likely that part of the precipitation on the mountains occurred as snow during the January 1989 event. However, we do not have observed snow height data. The WRF atmospheric forcing data, which was used coupled with the observed precipitation, slightly underestimates the temperature on the top of the mountains (i.e., the model is colder than reality). Thus, it does not seem to be a modelled temperature issue. The land surface model converts precipitation into snow and snow into melt water through a radiation- and temperature-based routine. The simulated snow depth and snow-water equivalent during the event of January 1989 might be lower than expected. Another indication sustaining this hypothesis is that for the event of November 1994 the model slightly underestimates the hydrograph peak. Details regarding how we modified the manuscript to incorporate these analyses are given in the answers to the specific comments.

Minor/specific comments

1. Abstract: stating that "few studies evaluate the hydrologic performance etc. . . ." is a bit debatable concept (e.g., few with respect to what?). This statement is different from a similar one on L81, where the authors specify that they are referring to WRF-Hydro. I would start the manuscript with a stronger sentence. Furthermore, in the Abstract the fact that 1989 events are used for calibration and 1994 events for validation should be stated more clearly.
   We have modified the first sentence of the abstract and have added the reference to calibration and validation for the two events of January 1989 and November 1994 as follows.

   Abstract, Line 12-13: "Coupled atmospheric-hydrologic systems are increasingly used as instruments for flood forecasting and water management purposes, making the performance of the hydrologic routines a key indicator of the model functionality".

   Abstract, Line 19-20: "Streamflow was modelled during extreme rainfall events that occurred in January 1989 (calibration) and November 1994 (validation) over 22 mountain watersheds".

2. L46 (and throughout the text): I would write "As summarized by Rummler et al. (2019)" rather than "As summarized by (Rummler et al., 2019)".
   Thanks for spotting it, we modified as suggested and we searched for similar occurrences throughout the manuscript.

3. L85: it looks like the events are much shorter. Including the spin-up period in this time interval could be misleading.
   To clarify this point, we modified the manuscript as follows.

   Introduction, Line 89-95: "The focus is on two extreme events that occurred over 22 small watersheds, located in the Troodos Mountains of Cyprus, between 8-10 January 1989 and 20-22 November 1994. The main objectives are: (i) to calibrate the uncoupled WRF-Hydro model for simulating extreme events in Cyprus with observed precipitation; and (ii) to evaluate the model performance when forced with WRF-downscaled (1 × 1 km^2) re-analysis precipitation data (ERA-Interim). The model runs covered two 15-day periods (1-16 January and 11-26 November) to include a short spin-up of the WRF-Hydro routines and the simulation and evaluation of the receding limb of the hydrograph".

4. Fig. 1: I suggest the authors focus more on the WRF-Hydro domain, which could be represented with a larger scale (so that also other information, e.g., location of raingauge stations and reservoirs, can be added). Location of the WRF-Hydro domain in Cyprus island could be shown with another small map in the figure.
   We have modified Fig. 1 according to the suggestions.

5. Table 1: A clear geological description is ok, but I would also highlight some essential geographical/morphological features, such as area, channel length, etc. Maybe authors can move some piece of information from Table 4 or just repeat it.
   We added area and channel length in Table 1 and left all the other variables in Table 4 as they were in the previous version of the manuscript.

6. L121: the problem of getting a reliable rating curve is rather common. More details about the "appropriate" rating curves used would be useful.
   We have added the following.

   Data, section 3.1 streamflow data, Line 124-130: "For the 22 watersheds, daily discharge data (m^3 s^{-1}) from streamflow stations of the Cyprus Water Development Department for the period 1980-2010 were analyzed. In addition, the original continuous hydrograph charts (water levels) of 16 of the 22 streamflow stations from the Water Development Department, for the Jan-1989 and Nov-1994 events, were scanned and manually digitized through the GetData Graph Digitizer software (http://getdata-graph-digitizer.com). The digitized water levels were interpolated to obtain values precisely every 15 minutes (00.00, 00.15, 00.30, 00.45, 01.00….) and converted to discharge with the appropriate rating curve of the station. The streamflow stations and rating curves are maintained by the Water Development Department through frequent observations".

7. Eq. 6: the variable Z should be explicitly defined
   We have added an equation (eq. 7) to define Z. The manuscript has been modified as follows.

Modelling setup, section 4.1 WRF-Hydro model description, Line 208-218: "The second solution consists of calculating a baseflow discharge [m^3 s^{-1}] (Q_{bf}) by means of an exponential bucket model, described by the following equation:

$$Q_{bf} = C \cdot \left(e^{a \cdot \frac{Z}{Z_{max}}} - 1\right), \quad (6)$$

where C is the bucket coefficient [m^3 s^{-1}], a is the bucket model exponent [-], Z_{max} is the maximum bucket level [m], and Z [m] is the bucket level at a certain time step. The user defines the C, a and Z_{max} parameters for each sub-watershed, together with a Z_{ini} [m] parameter to initialize the water storage in the bucket groundwater reservoir. At each time step the Z value is updated first adding the deep drainage contribution ($Perc$) and subsequently subtracting Q_{bf}:

$$Z_t = Z_{t-1} + \sum_{n=1}^{n=ncells} Perc_n - \frac{Q_{bf} \cdot DT \cdot 3600}{A} \quad (7)$$

where A is the area of the sub-watershed [m^2], DT the model time step [day], n is the index for the sub-watershed cells, and ncells represents the number of cells of the sub-watershed. Similar to the first solution, Q_{bf} is equally redistributed to channel segments. If Z equals or exceeds Z_{max}, all deep drainage is transferred to the channel network".

8. L218: information about average soil moisture would make more sense if information about soil type was provided

   We have modified the manuscript specifying the soil type as measured during experiments. Also, we added how we modified the original MODIS soil map to take into consideration the high permeable soils of the upper mountains (see also answer to general comment 3):

   Methods, section 4.2 WRF-Hydro Parameterization, Line 234-242: "Experimental data (Camera et al., 2018) show that in these conditions soil moisture for a gravelly sandy loam at 1300 m a.s.l. in the Troodos Mountains can vary between 0.10 and 0.15 m^3 m^{-3}. Therefore, the WRF-derived initial soil moisture values for November were halved.
   Land use and vegetation cover data were derived from the MODIS dataset through the WRF Pre-Processing System. According to the MODIS dataset, the Troodos Mountains has a uniform clay loam texture. However, field observations at higher elevation in the mountains, where the predominant lithologies consist of gabbro and ultramafic rocks, showed a gravelly sandy loam texture (Djuma et al., 2020; Camera et al., 2018; Cyprus Geological Survey Department, 1995). In addition, it is known that the Troodos gabbro is very weathered and therefore permeable (Christofi et al., 2020). Therefore, a sandy loam soil type was assigned to these areas.".

9. L228: 1500 cells should be 1500 x 100 x 100 = 15M m^2, that is 15 km^2 (it should be better stated explicitly). However, in Table 4 there are some catchments with area lower than this threshold.

   Right, that data was wrongly reported. The threshold is 250 cells (2.5 km^2). It is now clearly stated in the manuscript.

   Methods, section 4.2 WRF-Hydro Parameterization, Line 245-246: "For the channel grid, a flow accumulation threshold of 1500 250 cells (2.5 km^2) was adopted".

10. L267: at a time

Modified as:

Methods, section 4.2 WRF-Hydro Parameterization, Line 265-267: "The initial level of the conceptual reservoir (Z_{ini}) was set as a fraction of the maximum level (Z_{max}), based on the saturation degree of the deepest soil layer at the end of the 15-day WRF spin-up period".

11. Fig. 4 and elsewhere: to compare the performances of the model system for the two events, probably percent bias and MAE are more appropriate indices

We have modified Fig. 4, Fig. 7, and Fig. 8 substituting BIAS with percent bias (PBIAS). Figure numbering changed because we added a new Fig. 4 for the sensitivity analysis results, so they are now Fig. 5, Fig. 8, and Fig. 9.

12. LL320-333: [this comment refers to the main comment about dealing with rock fractures] from this paragraph, it's not clear if the problem is mainly related to the snow model in the LSM or the not good representation of the geological features. I would favour the second hypothesis, and I think that some test should be performed (and shown) by the authors increasing drainage.

As explained in the answer to the general comment 3, we have modified the parameter controlling deep drainage and the soil type based on geology (increased deep drainage and coarser soil for areas with gabbro and ultramafic rocks). We have incorporated in the sensitivity analysis one run with the modified deep drainage and three runs with different saturated hydraulic conductivity values, relative to different soil textures in the soil parameter tables. We have noticed a high sensitivity of saturated hydraulic conductivity and a rather low sensitivity of the deep drainage parameter. In the final model parameterization, we considered the results of the sensitivity analysis. In detail, we modified the manuscript as follows.

Methods, section 4.2 WRF-Hydro Parameterization, Line 237-254: "Land use and vegetation cover data were derived from the MODIS dataset through the WRF Pre-Processing System. According to the MODIS dataset, the Troodos Mountains has a uniform clay loam texture. However, field observations at higher elevation in the mountains, where the predominant lithologies consist of gabbro and ultramafic rocks, showed a gravelly sandy loam texture (Djuma et al., 2020; Camera et al., 2018; Cyprus Geological Survey Department, 1995). In addition, it is known that the Troodos gabbro is very weathered and therefore permeable (Christofi et al., 2020). Therefore, a sandy loam soil type was assigned to these areas. The related properties were attributed through the default table values implemented in WRF-Hydro (see Gochis et al., 2015). The hydrologic input layers (latitude, longitude, topography, flow direction, channel grid, lake grid, stream order, watersheds) were all calculated in ArcGIS® 10.2.2 starting from a 25 × 25 m^2 Digital Elevation Model (see Camera et al., 2017), resampled on the 100 × 100 m^2 grid, and the known locations of stream gauges and lakes. For the channel grid, a flow accumulation threshold of 250 cells (2.5 km^2) was adopted.

For the definition of the deep drainage related parameter, two approaches were tested. First, nine slope terrain classes were derived following Silver et al. (2017). In the second case, for cells where

the bedrock consists of gabbro or ultramafic rocks (Cyprus Geological Survey Department, 1995), the slope terrain class (3) that maximizes drainage (representing a highly fractured system) was assigned. In both cases, for each slope terrain class, the related default SLOPE value listed in the WRF-hydro general parameters table was given. These changes in soil type and deep drainage based on geology affected mainly watersheds Ma, An, Pl, Ka, and At, where 70% or more of the surface bedrock is made up of gabbro and ultramafic rocks (Table 1)".

Methods, section 4.3 WRF-Hydro Sensitivity Analysis, Line 269-277: "A sensitivity analysis of the LSM parameters REFKDT, SLOPE, and soil depth (SD), which have been identified as sensitive parameters in previous studies (e.g., Fersch et al., 2019; Senatore et al., 2015), was performed for the Jan-1989 event. In addition, sensitivity runs for the OVRGH parameter and the saturated hydraulic conductivity (K_S) were performed, too. For these simulations, the baseflow routine was switched off. A reference scenario was set, with REFKDT and OVRGH equal to 1, SD equal to 1.0 m, K_S equal to 2.45E-6 m s^{-1} (value attributed to clay loam soils in the soil parameter table), and the deep drainage parameter (SLOPE) assigned based on terrain slope, as in Silver et al. (2017). Parameters were changed one at a time. Eight values were tested for REFKDT (0.3, 0.5, 3.0, 5.0, 8.0, 10.0, 100.0, 1000.0), two for SD (0.5 and 2.0 m), two for OVRGH (0.1, 0.5), three for K_S (3.38E-6 m s^{-1} as for loam, 5.23E-6 m s^{-1} as for sandy loam, 1.41E-5 m s^{-1} as for loamy sand), and a different set of SLOPE values was assigned based on terrain slope and geology".

Methods, section 4.4 WRF-Hydro calibration and validation with observed precipitation, Line 296-297: "SLOPE parameters were assigned using the slope terrain class map allowing the best performance during sensitivity."

Results, section 5.1 sensitivity analysis, Line 344-349: "More sensitive than OVRGH is Ks, suggesting a possible important impact of the soil type and property definitions on the model output. Senatore et al. (2015) presented one of the few WRF-Hydro studies that calibrated a hydraulic conductivity related parameter, although they focused on the saturated soil lateral conductivity. SLOPE appeared to have a low sensitivity, although in the mountain watersheds, where it changed, a small reduction in the total discharged volume was observed".

Results, section 5.2 WRF-Hydro calibration and validation, Line 363-365: "SLOPE attributed based on both terrain slope and geology resulted in slightly better performance indices in the mountain watersheds than SLOPE attributed through terrain slope only. Therefore, it was selected for the final parameterization".

Results, section 5.2 WRF-Hydro calibration and validation, Line 380-389: "The parameterization of watersheds Ma, An, Pl, Ka, and At is peculiar. These watersheds are mainly characterized by sandy loam texture (i.e., higher Ks than the other watersheds), maximum deep drainage obtained by using the SLOPE parameters based on slope terrain and geology, very high REFKDT values, and very large groundwater storage. However, poor model fit indices (for some watersheds even negative) were obtained for the calibration period (Fig. 5). Conversely, the same watersheds show positive *NSE* values and negative *PBIAS* (i.e., slight underestimation of the peak discharge), for the validation event. Overestimation of runoff in Jan 1989 could have been

related to the modeling of snow and snowmelt in the LSM. Both observed and modeled temperature values for the upstream areas of these watersheds showed negative values, indicating that part of the precipitation was snow".

Conclusion, Line 533-534: "Modifications of deep drainage coefficients and MODIS soil types based on geology reduced the peak flow overestimation by up to 40% in watersheds characterized by a fractured and very permeable bedrock".

Conclusion, Line 539-544: "Negative *NSE* values were found in three watersheds located at high elevation where an underestimation of the snow fraction, computed by the LSM, may have occurred. Modelled snow height, and possible improvements deriving from the use of alternatives routines (e.g. Noah MP), should be checked with observed snow depth data, which were not available for this study".

Conclusion, Line 559: "Soil properties could be specifically calibrated for the study area".

13. LL335-339 and Figs. 5-6: the Y scale for watershed Mk is not appropriate (much higher maximum value than needed). The comment about watershed St does not correspond to what I can see in the Figures.
We modified the Y-scale of Mk in all figures and the comments related to both watersheds as follows.

Results, section 5.2 WRF-Hydro calibration and validation, Line 404-409: "Mk is the only watershed showing higher rainfall and flow peaks towards the end of the Jan-1989 event rather than in the middle. The model slightly underestimates the flow peak occurred on January 9th and overestimates the flow at the end of the simulation period. For St, the model reacts sharply to precipitation input, simulating well the flow peak occurred on January 9th but overestimating the flow at end of the simulation period of the Jan-1989 event and above all the peak of the Nov-1994 event, therefore affecting the performance scores".

14. L343: [this comment refers to the main comment about the groundwater bucket model] For Ak, it's not a problem of baseflow, but of recession, which is typically a problem concerning especially interflow (i.e., quicker contribution than baseflow).
Our bedrock is very fractured without a continuous groundwater table and we have predominantly shallow soils. It is difficult to distinguish between interflow and baseflow. We have observed slow dripping from the bedrock into upstream channels after large rainfall events. We also have streams that discharge to the bedrock with streamflow again recurring further downstream. Thus, we do have a streamflow recession made up of a combination of processes. As noted in general comment nr. 2, the OVRGH parameter influences the total discharged volume but not the shape of the hydrograph. Therefore, to better fit the post-peak shape of the hydrograph, we focused on baseflow calibration. To monitor the baseflow effect, we added four figures as supplementary material (Fig. S1 – S4), in which we showed the hydrographs for all watersheds together with the baseflow contribution, for both events and both observed and modelled rainfall as forcing. Fig. S1 and Fig. S3 show hydrographs for Jan-1989 event forced with

observed and modelled rainfall, respectively. Fig. S2 and Fig. S4 show hydrographs for Nov-1994 event forced with observed and modelled rainfall, respectively. To incorporate these analyses, we modified the manuscript as follows.

Methods, section 4.2 WRF-Hydro Parameterization, Line 255-258: "Other general parameters are REFKDT and soil depth (SD), which were calibrated. REFDK was left to its default value (2.00E-6 m s^{-1}). The WRF-Hydro parameter OVRGH was tested and values were assigned based on the sensitivity analysis, whereas RTDPT was kept constant all over the study area and a value of 1, consistent with a steep mountainous terrain, was assigned".

Methods, section 4.3 WRF-Hydro Sensitivity analysis, Line 271-277: "In addition, sensitivity runs for the OVRGH parameter and the saturated hydraulic conductivity (K_S) were performed, too. For these simulations, the baseflow routine was switched off. A reference scenario was set, with REFKDT and OVRGH equal to 1, SD equal to 1.0 m, K_S equal to 2.45E-6 m s^{-1} (value attributed to clay loam soils in the soil parameter table), and the deep drainage parameter (SLOPE) assigned based on terrain slope, as in Silver et al. (2017). Parameters were changed one at a time. Eight values were tested for REFKDT (0.3, 0.5, 3.0, 5.0, 8.0, 10.0, 100.0, 1000.0), two for SD (0.5 and 2.0 m), two for OVRGH (0.1, 0.5), three for K_S (3.38E-6 m s^{-1} as for loam, 5.23E-6 m s^{-1} as for sandy loam, 1.41E-5 m s^{-1} as for loamy sand), and a different set of SLOPE values was assigned based on terrain slope and geology".

Methods, section 4.4 WRF-Hydro calibration and validation with observed precipitation, Line 297-309: "REFKDT and OVRGH were initialized, in each watershed, based on the evaluation of the sensitivity runs through performance indices, as for SD. For the baseflow bucket routine, initial values of a and Z_{max} were set to the default. Next, the initialized parameters were fine-tuned based on a trial and error procedure for all watersheds. Modifications were applied to a single parameter at the time and if changes could not improve the model performance according to three indices out of five after five attempts, the parameters were retained. Commonly applied changes were ±1 for REFKDT, ±0.1 for OVRGH, ±0.5 for a, and ±10% of the actual value for Z_{max}. Smaller (larger) changes were applied only in watersheds where the response of streamflow was (not) particularly sensitive to specific parameters. The parameterization of Z_{max} was aimed at filling the reservoir after the rainfall peak, between 10 January at midnight and 11 January at noon, to simulate the observed recession of the hydrograph. For those watersheds that highly overestimated the baseflow due to spilling out of the groundwater reservoir, Z_{max} was further increased. A good fit between observed and simulated flow before the peak was the target for the calibration of the exponent α".

Results, section 5.1 sensitivity analysis, Line 344-348: "Regarding OVRGH, results show that it has a slight control on the total volume discharge, as also presented in Yucel et al. (2015), while it has almost no effect on delaying the peak (Fig. 4). More sensitive than OVRGH is Ks, suggesting a possible important impact of the soil type and property definitions on the model output. Senatore et al. (2015) presented one of the few WRF-Hydro studies that calibrated a hydraulic conductivity related parameter, although they focused on the saturated soil lateral conductivity".

Results, section 5.2 WRF-Hydro calibration and validation, Line 365-368: "Also, for all watersheds OVRGH was set equal to 1 because it was the value returning the best performance indices in 19 out of 22 watersheds. Furthermore, considering that OVRGH effects total discharge volume and not hydrograph shape, its calibration would have been equifinal to REFKDT".

Results, section 5.2 WRF-Hydro calibration and validation, Line 418-423: "As it is visible in Fig S1 and Fig S2, flow in the receding limb of the hydrograph is mainly made up of baseflow. For Jan-1989 event, in all these watersheds the groundwater reservoir is filled up on January 10th and baseflow consists of the water spilling out from it. This water volume, redistributed along the channel network, is generally able to reproduce the hydrograph shape, except in Ak. In Nov 1994, no groundwater spilling is observed during the simulation and the receding limb is underestimated. Therefore, this could be partly due to a non-perfect reproduction of the model initial conditions and partly related to an underestimation of interflow and baseflow".

Conclusion, Line 535-537: "The overland roughness routing factor reduced the streamflow but showed a very limited effect on delaying flow. A straightforward calibration of the baseflow reservoir based on low flow fitting (exponent) and reservoir filling time (maximum capacity) was a good mean for obtaining a reasonable simulation of the hydrograph recession in most watersheds".

Conclusion, Line 560-561: "For a continuous, long-term streamflow analysis, an evaluation of the sensitivity of the baseflow reservoir parameters could be carried out.".

15.L344: the peak looks not so well simulated in Ak

We agree. We have modified the manuscript as follows.

Results, section 5.2 WRF-Hydro calibration and validation, Line 410-418: "In the eastern part of the modelling domain (La to Ni), for the calibration event both initial baseflow and the discharge peak are well modelled in all watersheds (Fig. 6). Differences between observed and simulated hydrographs can be observed in the post-peak, for watersheds Ak, Pe (Fig. S1), Ko and Ni. Ak and Pe present a very high peak flow (> 50 $m^3 s^{-1}$) and an underestimation of the receding limb of the hydrograph in the following days, which causes the negative *PBIAS* and high *MAE* values visible in Fig 5. In the case of Ko and Ni, the receding limb shows a little overestimation. For the validation event (Fig. 7), the peak is well simulated in Pe and Ao, slightly overestimated in Ak and Pd, underestimated in La, Vy, Ko, and Ni (Pe and Pd, Fig. S2). In the post peak phase, the simulated hydrographs show negative biases in comparison to the observed ones in all watersheds".

16.L368: passing -> moving?

Modified as suggested.

17. LL372-374: these sentences are confusing, especially if compared with LL351-353, which seem to refer to the same comparison. Not clear what the authors mean when they state that bias "on average increased by 8.6 times"

The first lines described rainfall, while the second group described streamflow. Throughout section 5.3 we have now modified the text so that it is explicitly said if the performance indices refer to precipitation or streamflow. We introduced PBIAS as a replacement of BIAS so we modified the unclear sentence.

Line 461-463: "The absolute value of flow *PBIAS* decreased in seven watersheds (Af, Li, Pl, Vy, Ak, Ko, Ni) but on average increased by 21.5% (96.6% in Pg and 120.3% in Le)".

18. L395: the three watersheds

Thanks for spotting it. Changing some parameter during calibration the watersheds became four (**Line 495** in the manuscript with track changes).

19. L400: decent -> reasonable? Besides, again I don't think it's a matter of baseflow

We modified the text discussing the receding limb of the hydrograph in general and not baseflow only.

Results, section 5.4 WRF-Hydro with observed and modeled precipitation evaluation at hourly scale, Line 500-503: "In addition, the receding hydrograph is well modelled for the calibration event but not so well for the validation event. This result is similar to what was observed for daily streamflow and was attributed to the possible non-perfect reproduction of the model initial conditions and underestimation of interflow. The fairly good post-peak simulations lead to reasonable hourly performance indices for the Jan-1989 event.".

20. L412: probably, increasing overland roughness coefficient could be also a way for improving interflow and, therefore, the simulation of the falling limb of the hydrograph

Please refer to answer to previous comments regarding overland roughness and interflow (general comment 2, minor comments 14, 15, 19).

21. LL442-443: please contextualize better this sentence

We have modified the sentence.

Conclusion, Line 551-557: "This suggests that model calibration with modelled rainfall forcing is not optimal for small mountain watersheds and should be carefully evaluated if no other options are available. As a consequence, WRF rainfall forecasts may not be sufficiently accurate for predicting the location and size of specific floods of such small mountain watersheds. However, due to the relatively small errors in total precipitation (average relative difference over the 22 watersheds of 17% and for 20% Jan 1989 and Nov-1994 events, respectively) and simulated daily maxima (average relative difference over the 22 watersheds of 22% and 18% for Jan 1989 and Nov-1994 events, respectively), modelled rainfall data could be suitable for investigating the effect of climate change on extreme rainfall and flood events".

Anonymous Referee #2

This paper presents a modeling work on 22 small watersheds using WRF-hydro. The model is forced with modeled WRF data and observe precipitation for 2 periods in January 1989 and November 1994. The authors concluded that using WRF precipitation may not be suitable for hydrological studies in small mountain basins although they are still useful for long term studies.

General comment

1. I am not quite sure what is the research question that the authors are trying to answer. If it is WRF-hydro ability to simulate streamflow, I think that is widely covered in the literature review, but it may be important a benchmarking in this specific area. If it is the advantage of using observed precipitation, I think that it is not necessary to write a paper about it since it is well known that if there are observations available, it is better to use them over modeled data or to correct the modeled data. Therefore, it is not clear to me what is the actual contribution that the authors are trying to deliver. The problem with modeled precipitation is because the WRF model does not work? Or the modeler did not implement it correctly? When the model and observe precipitation does not compare well, why did you use it anyway? I think that using incorrect input will certainly result in poor performance. But jumping from there to conclude that we should not use modeled precipitation is a big stretch. I think that the paper should focus on the performance of WRF-hydro. The model performance is not affected if the precipitation is observed or modeled since you are using it uncoupled.

   We used the best possible approach to model convective rainfall events and the results obtained show a good agreement with the observed fields. They compare well. Therefore, we consider our modelled rainfall input as a sub-optimal input. Although the high quality of it, still the small errors in the rainfall, in such small watersheds, propagate in the streamflow deeply affecting the performance. We have modified the introduction and the conclusion to state in a clear way that the value of the results is limited to small watershed (below 100 km^2) and that model calibration carried out with modelled data is not optimal, not that it shouldn't be performed at all. Also, we suggest that WRF rainfall forecasts may not be sufficiently accurate for predicting the location and size of the floods of such watersheds thinking of implementing a similar system as an operational flood forecasting tool.

   Introduction, Line 87-89: "Model performance loss due to differences between observed and modelled rainfall is rarely discussed. Also, little attention has been given to small watersheds (area below 100 km^2), which are often ungauged and prone to flash floods. This study aims to address this gap".

   Conclusion, Line 523-527: "This study evaluates streamflow simulations of the one-way coupled atmospheric-hydrologic model WRF-Hydro, forced with observed and WRF-modeled rainfall, during two extreme events, over 22 small mountain watersheds in Cyprus (area below 100 km^2). Following model calibration and validation with observed rain, the model was run with WRF-downscaled (1 × 1 km^2) re-analysis precipitation data (ERA-Interim). These forcing data represent best-performing hindcasts of two extreme rainfall events, i.e. a model product that is as similar as possible to reality and considered sub-optimal".

Conclusion, Line 551-557: "This suggests that model calibration with modelled rainfall forcing is not optimal for small mountain watersheds and should be carefully evaluated if no other options are available. As a consequence, WRF rainfall forecasts may not be sufficiently accurate for predicting the location and size of specific floods of such small mountain watersheds. However, due to the relatively small errors in total precipitation (average relative difference over the 22 watersheds of 17% and for 20% Jan 1989 and Nov-1994 events, respectively) and simulated daily maxima (average relative difference over the 22 watersheds of 22% and 18% for Jan 1989 and Nov-1994 events, respectively), modelled rainfall data could be suitable for investigating the effect of climate change on extreme rainfall and flood events".

Specific Comments

1. First line abstract: "Few studies evaluate the hydrologic performance of coupled atmospheric-hydrologic models when forced with observed rainfall and even fewer when forced with modeled precipitation." This is not quite true, there is extensive literature on this topic. If you are specifically referring to WRF-hydro you should state that.
   We have modified the first sentence of the abstract as follows.

   Abstract, Line 12-13: "Coupled atmospheric-hydrologic systems are increasingly used as instruments for flood forecasting and water management purposes, making the performance of the hydrologic routines a key indicator of the model functionality".

2. The first paragraph of the introduction is related to the land-atmosphere feedbacks, which is not the case of this study, so I suggest eliminating it or to refocus it to the topic of the paper
   We have refocused the paragraph to the topic of the paper by adding a sentence at the end of it.

   Introduction, Line 39-40: "However, recently authors have started to see these systems as instruments for flood forecasting, making the performance of the hydrologic routines a key indicator of the model quality (Givati et al., 2016; Maidment 2017)".

3. What about the bucket model parameter sensitivity? There is no indication of the interaction of those in the uncertainty analysis.
   Yes, good point. We conducted the sensitivity analysis on the parameters mainly influencing the rainfall runoff-infiltration partitioning (including few sensitivity runs regarding the overland roughness coefficient that we added during the review), with the baseflow bucket model switched off. For the calibration, we found that we could improve the simulations with a straightforward tuning of the baseflow parameters based on its filling time and the fit of the pre-peak hydrograph. We agree that a sensitivity analysis of the baseflow parameters is useful, but it would be more suitable to do this for a continuous, long-term streamflow analysis. We have added a recommendation about this in the conclusions.

   Conclusion, Line 560-561: "For a continuous, long-term streamflow analysis, an evaluation of the sensitivity of the baseflow reservoir parameters could be carried out".

4. Is there any evaluation of precipitation disaggregation eq 1 and 2?

   We derived hourly fields with the presented disaggregation method and with simple IDW interpolation, since the method worked best for daily local events (Camera et al., 2014). We forced WRF-Hydro with both datasets and obtained a better fit of streamflow with the disaggregated one. In addition, looking at the 5-day cumulated rainfall fields calculated from the two hourly datasets, for the days around the peak precipitation for the two events of interest, we noticed a more plausible areal distribution for the disaggregation method (Fig. 1R). In addition, this method allows to preserve the mass balance between the daily and the hourly dataset. We did not include this explanation in the manuscript for conciseness.

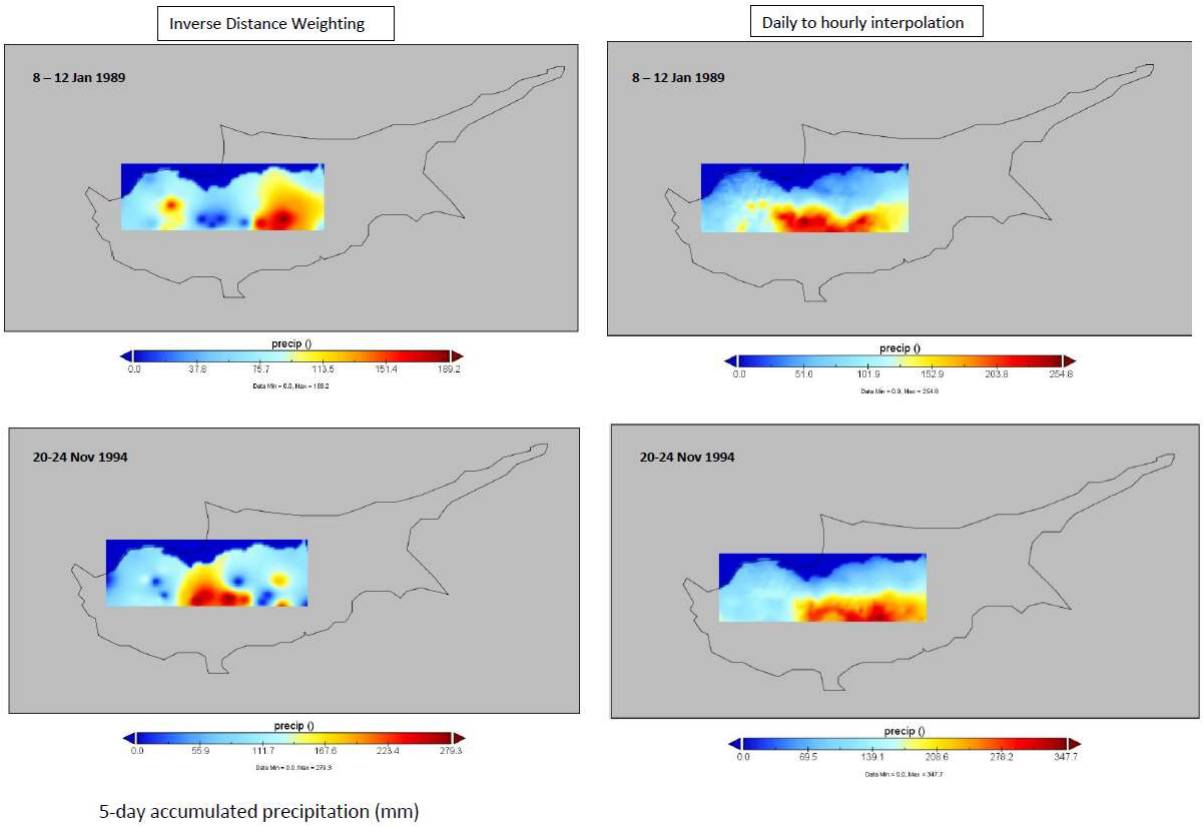

Fig. 1R: comparison of 5-day cumulated rainfall around the precipitation peak of the two events of interest (Jan 1989 and Nov 1994) obtained with two different interpolation methods, Inverse Distance Weighting (IDW) and disaggregation of daily to hourly values.

5. In Figure 4, there a series of inconsistencies between the performance of the model between the calibration and evaluation period. Is there any explanation for that? In particular basins, Ma, An, Pi, Ka, where you have really bad results during the calibration but still validate the models and got very good results.

   This relates to some of the comments Reviewer #1 made, too. For us, it is partly related to the geological characteristics of those watersheds and partly to the fact that they are located at high elevation and part of the precipitation during Jan-89 event occurred as snow. We managed to slightly improve the hydrograph simulation of these watershed (still they are not optimal)

modifying deep drainage and soil properties based on geology. We have modified the SLOPECAT map and consequently the SLOPE coefficients (controlling deep drainage) based on geology. For gabbro and ultramafic rock types we forced a SLOPECAT resulting in a SLOPE coefficient equal to 1 (i.e., the maximum possible value) and therefore a maximization of the drainage from the soil column to the groundwater bucket. Also, we modified the soil type of the area from clay loam (MODIS database) to sandy loam, based on field evidence. The overestimation of the peak got reduced up to 40% but still an overestimation remained. The same model parameterization results in positive NSE and negative BIAS for the Nov-1994 event. This combination of results led us to believe that the main issue is an underestimation of the snow. Please refer to the answers to the general comment 3 and specific comment 12 of Reviewer #1 for details on the added analyses and manuscript modifications.

6. Also, it would be better to use percentage bias instead of bias alone to have a more general indicator of biases.
   We modified the manuscript accordingly.

7. Figures 5 and 6, it is very hard to see the differences in precipitation. And then, why to use incorrect model precipitation at all.
   We changed the color of modelled rainfall, we hope figures are clearer than in the previous version. Figures numbering changed because we added an extra figure to discuss the sensitivity analysis results. The mentioned figures are now Fig. 6 and Fig. 7.
   Regarding rainfall, in our intention we do not use incorrect rainfall, we use the best available modelled rainfall. Please refer to the answer to your general comment 1.

8. If we look at figures 7 and 8, we can see that WRF-hydro does a really bad job (Figure 8) in basins where WRF precipitation has good performance (Figure 7), can you explain why?
   Fig. 7 and Fig. 8 are now Fig. 8 and Fig. 9. WRF-Hydro forced with modelled rainfall seems to poorly simulate especially watersheds Af (Nov 1994), Pg (both events), Le (both events), Mk (Jan 1989), Li (Nov 1994), An (Jan 1989), Pl (Jan 1989). For An and Pl, we believe that the problem is the same as for observed rainfall, therefore related partly to the difficult parameterization of a highly fractured bedrock and partly to the high elevation causing snow. Watershed Af, for Nov-1994 event show a very high rainfall PBIAS. Watershed Le shows rather low rainfall NSE for both events and a very high rainfall PBIAS for Jan-89 event. Watershed Li show a medium-high MAE for Nov-1994. Watersheds Pg and Mk are those characterized by the lowest average discharge during both events. Therefore, small discharge variations cause higher performance loss for them than for all other watersheds. They are the perfect exemplification of what we wrote in the manuscript about the small shifts in the space-time rainfall fields causing important performance losses. Figures S3 and S4 in the supplementary material show it. We have modified the manuscript as follows to stress this point.

   Results, section 5.3 WRF-Hydro simulations with modeled precipitation, Line 470-475:
   "These results indicate that a small shift in time or space of modelled rainfall, in comparison to

observed precipitation, can strongly modify the hydrologic response of small watersheds to extreme events. This is particularly evident in watersheds Pg and Mk, which are among the smallest and those characterized by the lowest average discharge in both events (Fig. 6, Fig. 7, Fig. S3, Fig. S4). Although their rainfall performance indices (Fig. 8) do not show particularly large errors (except a negative NSE for Mk in Nov 1994), streamflow fit indices present very negative values and streamflow PBIAS is very high as well (Fig. 9)".

9. In the conclusion you mention this "Streamflow obtained with WRF-modelled rainfall forcing showed high discrepancies with observations, despite the good agreement between modeled and observed precipitation (average NSE of 0.83 and 0.49 for Jan1989 and Nov 1994, respectively)." Did you try to calibrate the model with the modeled precipitation data and evaluate the observation?
   This is a good point. We thought about it during the design of the methodological approach but then we preferred to focus on the performance loss passing from a calibration on observed rainfall to a simulation with modelled rainfall. Also, we are aware that the observed gridded dataset could be characterized by errors but the high density of stations and the study done on the creation of the daily dataset, including the evaluation of the final product (Camera et al., 2014), gave us some confidence about the quality of the input data.

References not present in the manuscript

Simmons, A, Soci, C, Nicolas, J, Bell, B, Berrisford, P, Dragani, R, Flemming, J, Haimberger, L, Healy, S, Hersbach, H, Horányi, A, Inness, A, Munoz-Sabater, J, Radu, R, Schepers, D, 2020. Global stratospheric temperature bias and other stratospheric aspects of ERA5 and ERA5.1. ECMWF Technical Memoranda 859, Reading (UK), 40 pp.

Simulation of extreme rainfall and streamflow events in small Mediterranean watersheds with a one-way coupled atmospheric-hydrologic modelling system

Corrado Camera[1], Adriana Bruggeman[2], George Zittis[3], Ioannis Sofokleous[2], and Joël Arnault[4]

[1] Dipartimento di Scienze della Terra 'A. Desio', Università degli Studi di Milano, Milano, 20133, Italy
[2] Energy Environment and Water Research Center, The Cyprus Institute, Nicosia, 2121, Cyprus
[3] Climate and Atmosphere Research Center, The Cyprus Institute, Nicosia, 2121, Cyprus
[4] Institute of Meteorology and Climate Research, Karlsruhe Institute of Technology, Garmisch-Partenkirchen, 82467, Germany

Correspondence to: Corrado Camera (corrado.camera@unimi.it)

Abstract.

Coupled atmospheric-hydrologic systems are increasingly used as instruments for flood forecasting and water management purposes, making the performance of the hydrologic routines a key indicator of the model functionality~~Few studies evaluate the hydrologic performance of coupled atmospheric-hydrologic models when forced with observed rainfall and even fewer when forced with modelled precipitation. This information is crucial for the study of floods and in general for the use of the models for water management purposes~~. This study's objectives were: (i) to calibrate the one-way coupled WRF-hydro model for simulating extreme events in Cyprus with observed precipitation; and (ii) to evaluate the model performance when forced with WRF-downscaled (1 × 1 km^2) re-analysis precipitation data (ERA-Interim). This set up resembles a realistic modelling chain for forecasting applications and climate projections. Streamflow was modelled during extreme rainfall events that occurred in January 1989 (calibration) and November 1994 (validation) over 22 mountain watersheds. In six watersheds, Nash-Sutcliffe Efficiencies (NSE) larger than 0.5 were obtained for both events. The WRF-modelled rainfall showed an average NSE of 0.83 for January 1989 and 0.49 for November 1994. Nevertheless, hydrologic simulations of the two events with the WRF-modelled rainfall and the calibrated WRF-Hydro returned negative streamflow NSE for 13 watersheds in January 1989 and for 18 watersheds in November 1994. These results indicate that small differences in amounts or shifts in time or space of modelled rainfall, in comparison with observed precipitation, can strongly modify the hydrologic response of small watersheds to extreme events. Thus, the calibration of WRF-Hydro for small watersheds depends on the availability of observed rainfall with high temporal and spatial resolution. However, the use of modelled precipitation input data will remain important for studying the effect of future extremes on flooding and water resources.

1 Introduction

Atmospheric and hydrologic processes are strictly related, since they share the land surface as a common interface for moisture and heat fluxes. Precipitation is the primary cause of all surface hydrologic processes, such as overland, subsurface and river flow. Conversely, soil moisture and surface water distributions affect near surface atmospheric conditions and processes, such as the temperature distribution, the structure of the atmospheric boundary layer, the formation of shallow clouds and precipitation amounts (Lin and Cheng, 2016; Zittis et al., 2014 and references therein). In recent years, the scientific community has made ever-increasing efforts to improve the simulation skills of both atmospheric and hydrologic models, leading also to the development of coupled modelling systems. Since the beginning of the 21st century, the main research interest in developing such models has been the evaluation of the feedbacks between the hydrologic cycle and the atmospheric processes, to get a deeper understanding of regional climate change and its impacts (Ning et al., 2019). However, recently authors have started to see these systems as instruments for flood forecasting, making the performance of the hydrologic routines a key indicator of the model quality (Givati et al., 2016; Maidment, 2017).

The Weather Research and Forecasting hydrologic modeling system WRF-Hydro (Gochis et al., 2015) is an example of such a modelling system. It consists of a set of routines extending the hydrologic physics options in the Noah Land Surface Model (Noah LSM, Ek et al., 2003) and Noah with Multi-Parameterization Land Surface Model (Noah-MP LSM, Niu et al., 2011), which are the most commonly used land surface schemes of WRF (Constantinidou et al., 2019; Skamarock and Klemp, 2008). In relation to WRF, WRF-Hydro can be run in an uncoupled (one-way coupled) mode or in a fully-coupled (two-way coupled) mode. In the first case, WRF-Hydro is run with user's specified atmospheric forcing, which can be observations, reanalyses, previously calculated model outputs or a mixture of the three (e.g., observed precipitation and WRF-derived temperature, wind speed, humidity, radiation etc). As a result, hydrologic outputs are influenced by the atmospheric variables but not vice versa. In the second case, WRF-Hydro enhanced hydrologic routines update the land surface states and fluxes in the LSM grid, which are then used by the atmospheric component of the model.

As summarized by (Rummler et al., (2019), WRF-Hydro is mainly used in its uncoupled mode for model calibration and flood forecasting (e.g., Lahmers et al., 2019; Maidment, 2017; Silver et al., 2017; Verri et al., 2017; Givati et al., 2016; Yucel et al., 2015). Conversely, the fully-coupled mode is usually adopted to investigate land-atmosphere feedbacks (Arnault et al., 2016, 2019; Rummler et al., 2019; Senatore et al., 2015; Wehbe et al., 2019; Zhang et al., 2019).

Focusing on the use of the model for the simulation of flood events, (Yucel et al., (2015) calibrated WRF-Hydro over one watershed and two heavy rainfall events in northern Turkey, using 4-km WRF rainfall as input. The calibrated model parameters were then applied to three other watersheds and 10 heavy rainfall events. Their main aim was to quantify the performance improvement of the calibrated WRF-Hydro model against its use with default parameterization and test parameter transferability. In addition, they tested the model with WRF, WRF with data assimilation, and EUMETSAT precipitation derived input. They obtained the best results with the calibrated model, forced by WRF with data assimilation precipitation. They suggest that this model configuration allows parameter transferability to ungauged catchments.

(Givati et al., (2016) calibrated uncoupled WRF-Hydro based on gridded observations of two high intensity rainfall events that occurred in 2013 over the Ayalon basin in Israel. The calibrated model was subsequently run with WRF-derived precipitation resulting from both uncoupled and fully-coupled simulations. The study demonstrated that both precipitation and streamflow as derived from the fully-coupled model were superior to one-way coupled results, suggesting a possible application of fully coupled systems for early flood warning applications. Still, the authors suggested further research with a similar study set-up but over areas characterized by different precipitation and hydrologic regimes.

Silver et al. (2017) focused on five extreme events occurring over seven watersheds located in Israel and Jordan. They proposed a procedure for parameterizing the model scaling coefficients related to infiltration partitioning and soil hydraulic conductivity, as well as for defining topographic categories. The procedure was based on soil physical properties and terrain characteristics only. They demonstrated that their method leads to better streamflow predictions than trial and error calibration and is as good as expert knowledge parameterization.

Verri et al. (2017) calibrated an uncoupled WRF/WRF-Hydro modelling system over the Ofanto river basin, in southern Italy. Focus was on two three-month periods, each characterized by a heavy rainfall event and covering different seasons. WRF was run with 16-km horizontal resolution and 6-h fields forced by ECMWF-IFS (European Centre for Medium-Range Weather Forecasts – Integrated Forecasting System) as initial and boundary conditions. In addition, they presented a WRF rainfall correction approach based on rainfall observations, an objective analysis and a least square melding scheme and demonstrated that it improved river discharge simulation. The study also showed that optimal, calibrated values of infiltration partitioning and baseflow coefficients differ in the two events, suggesting a seasonal dependence.

Nowadays, uncoupled WRF-Hydro is the core of the National Water Model (NWM, https://ral.ucar.edu/projects/supporting-the-noaa-national-water-model), running over the Conterminous United States and furnishing streamflow forecasts for 2.7 million river reaches. The NWM flood forecasting skills has been strengthened within the framework of the National Flood Interoperability Experiment (Maidment, 2017). The NWM and WRF-Hydro remain under constant development. An

example is the study of (Lahmers et al., (2019), who added channel infiltration processes to the modelling system to improve streamflow simulations in the arid southwestern United States.

From this review, it appears that few studies focus on the evaluation of the hydrologic output of WRF-Hydro when forced with observed rainfall and just a few more when forced with modelled rainfall. Model performance loss due to differences between observed and modelled rainfall is rarely discussed. Also, little attention has been given to small watersheds (area below 100 km^2), which are often ungauged and prone to flash floods. This study aims to address this gap. The focus is on two extreme events that occurred over 22 small watersheds, located in the Troodos Mountains of Cyprus, between 18-106 January 1989 and 2011-226 November 1994. The main objectives are: (i) to calibrate the uncoupled WRF-Hydro model for simulating extreme events in Cyprus with observed precipitation; and (ii) to evaluate the model performance when forced with WRF-downscaled (1 × 1 km^2) re-analysis precipitation data (ERA-Interim). The model runs covered two 15-day periods (1-16 January and 11-26 November) to include a short spin-up of the WRF-Hydro routines and the simulation and evaluation of the receding limb of the hydrograph.

2 Study area

This study focuses on 22 watersheds located on the northern slope of the Troodos Mountains, Cyprus (Figure 1). The bedrock geology of the region is characterized by an ophiolitic complex. The highest peak of Troodos is Mt. Olympus (1952 m a.sl.). At high elevations (above 1400 m a.s.l.), ultramafic rocks are the dominant lithology (harzburgite, serpentinite, pyroxenite, wehrlite and dunite). Moving downhill, dominant rock types show a transition from gabbro to diabase, pillow lavas and sedimentary formations, therefore stratigraphically from the lower to the higher lithotype. Between gabbro and pillow lavas, diabase is present in the form of sheeted dykes and it constitutes the largest area of Troodos outcrop. Often, pillow lavas and sheeted dykes do not present a net geological limit, but the oldest lavas host the youngest dykes (Cleintaur et al., 1977). This transitional zone between pillow lavas and dykes takes the name of basal group. Throughout the ophiolitic complex, bedrock is usually found at shallow depths. According to the digital soil map of Cyprus (Camera et al. 2017), most of the soils over Troodos are Lithic Leptosols with a stony gravelly texture and a predominant very shallow depth (0-10 cm), which can sometimes reach up to 100 cm. These characteristics highlight why rock fractures can be considered the main controlling factor for the region's subsurface hydrology.

Due to its characteristic Mediterranean climate, more than 90% of a hydrologic year's (October-September) runoff from Troodos is produced between December and April. During the summer months, most rivers are completely dry (Le Coz et al., 2016). Due to their small areas and steep slopes, all watersheds have quite short times of concentration. Therefore, intense rainfall events lasting few hours can easily cause floods in the downstream plains.

Table 1 lists the 22 watersheds, their area and the total modeled stream length, and summarizes their geology, as obtained from the geological map of Cyprus (Cyprus Geological Survey Department, 1995). Agios Nikolaos and Platania are sub-watersheds of Kargiotis; Lagoudera is a sub-watershed of Vyzakia; Kotsiati is a sub-watershed of Nisou.

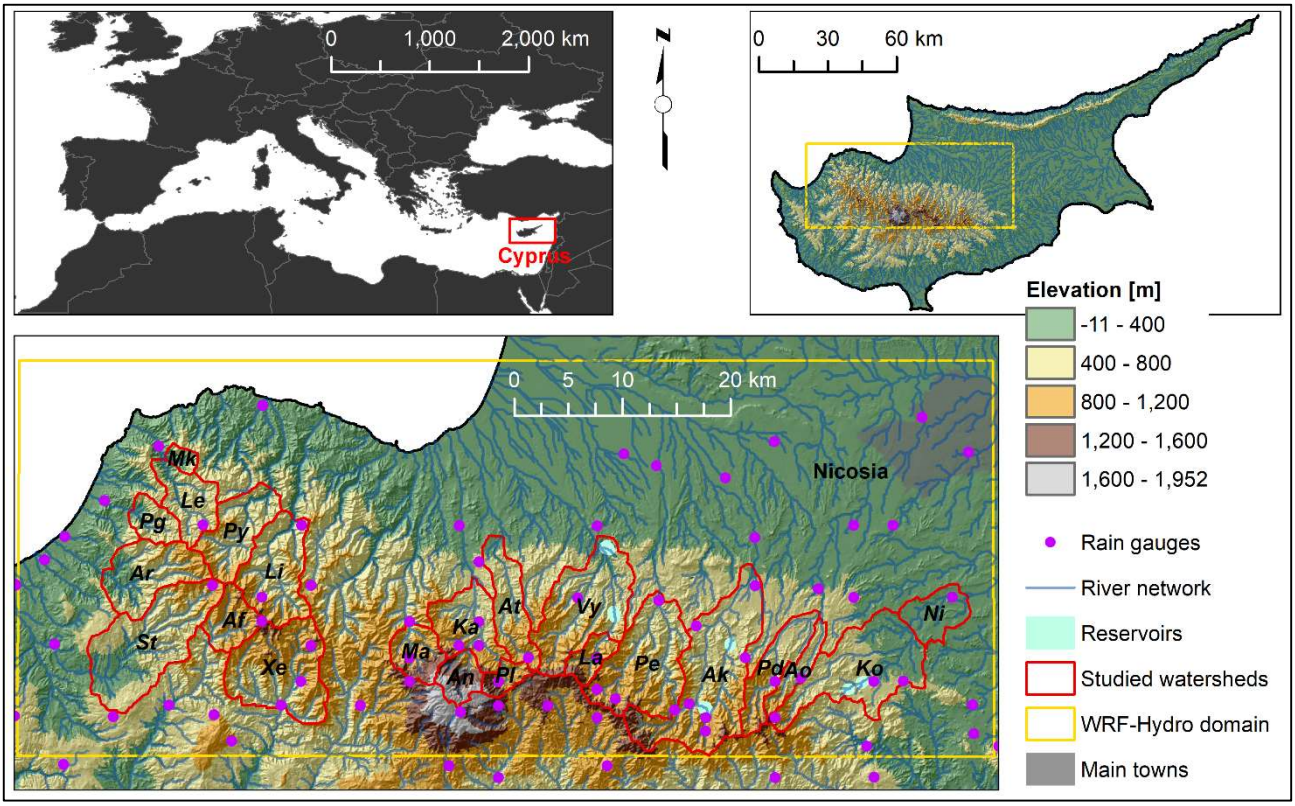

Figure 1. Geographical setting of the island of Cyprus and WRF-Hydro study area with the 22 target watersheds. For watershed short names refer to Table 1.

120

Table 1. Morphological and Geological characteristics of the studied watersheds.

Watershed	Watershed short name	Area [km^2]	Channel length [km]	Ultramafic complex [%]	Gabbro [%]	Sheeted Dikes [%]	Basal group [%]	Pillow Lavas [%]	Sedimentary formations [%]
Xeros	Xe	67.5	11.0	0	0	100	0	0	0
Agia Forest	Af	21.3	5.5	0	0	100	0	0	0
Stavros	St	78.9	18.9	0	0	42	13	0.17	26
Argaka	Ar	44.7	11.9	0	0	72	24	0.04	0
Pano Gialia	Pg	15.1	4.9	0	0	100	0	0	0
Leivadi	Le	27.9	8.8	0	4	96	0	0	0
Mavros Kremnos	Mk	5.2	2.0	0	8	92	0	0	0
Pyrgos	Py	38.1	12.0	0	0	100	0	0	0
Limnitis	Li	48.0	11.5	0	0	100	0	0	0
Marathasa	Ma	22.6	5.4	15	65	20	0	0	0
Agios Nikolaos	An	15.7	4.8	95	5	0	0	0	0
Platania	Pl	10.2	2.1	33	67	0	0	0	0
Kargiotis	Ka	64.6	13.1	30	41	25	3	1	1
Atsas	At	32.7	15.8	0	47	42	8	3	0
Lagoudera	La	14.5	4.9	0	12	76	11	0	0
Vyzakia	Vy	81.0	15.6	0	11	36	38	14	0
Peristerona	Pe	78.2	13.2	1	11	69	20	0	0
Akaki	Ak	96.7	25.0	0	2	37	47	11	2
Agios Onoufrios	Ao	14.2	11.0	0	0	33	57	9	0
Pedieos	Pd	29.8	16.5	0	0	52	35	11	1
Kotsiatis	Ko	74.1	21.3	0	1	11	28	59	1
Nisou	Ni	95.6	30.3	0	0	9	22	50	18

3 Data

3.1 Streamflow data

For the 22 watersheds, daily discharge data (m^3/s^{-1}) from streamflow stations of the Cyprus Water Development Department for the period 1980-2010 were analyzed. In addition, the original continuous hydrograph charts (water levels) of 16 of the 22 streamflow stations ~~from the Water Development Department~~, ~~for the~~ for the Jan-1989 and Nov-1994 events, were scanned and manually digitized through the GetData Graph Digitizer software (http://getdata-graph-digitizer.com). The digitized water levels were interpolated to obtain values precisely every 15 minutes (00.00, 00.15, 00.30, 00.45, 01.00….) and converted to discharge with the appropriate rating curve of the station. The streamflow stations and rating curves are maintained by the Water Development Department through frequent observations. Both interpolation and conversion were carried out by R scripts (https://www.r-project.org/). The 15-minute data were aggregated into hourly discharge values. Both hourly and daily values were used for model performance analysis.

3.2 Meteorological data

An hourly gridded dataset with a resolution of 1×1 km^2 was developed using hourly and daily rainfall data from the Cyprus Department of Meteorology stations and the daily gridded rainfall dataset of Camera et al. (2014). Data were extracted for two extreme events, with 42 rain gauges available over the island for Jan 1989 and 37 rain gauges available for Nov 1994. The temporal disaggregation from daily to hourly gridded rainfall was developed through a FORTRAN code based on the method of hourly fractions (Di Luzio et al., 2008), which preserves the original daily values. The main steps of the disaggregation method are:

a. The hourly rainfall observations (*ph*) are summed in 24-hour totals (*phs*). The 24-hour period ranges from 8.00 AM of the previous day until 8.00 AM of the attribution day, coherently with the daily gridded dataset.
b. The fractions of the hourly rainfall data to the daily total rainfall are calculated as:

$$hfrac = ph/phs. \quad (1)$$

c. The nearest gauge to each rainfall gridded dataset cell (*ng*) is found.

d. The hourly rainfall at each grid cell (*phc*) is calculated by multiplying each gridded daily (*d*) rainfall value (*pdc*) with the hourly (*h*) fraction (*hfrac*) of the nearest valid gauge (*ng*).

$$phc(h,ng) = pdc(d,c) \cdot hfrac(h,ng). \quad (2)$$

4 Modelling setup

4.1 WRF-Hydro model description

The WRF-Hydro model is an extension package of the 1-D Noah LSM and Noah-MP LSMs, which are commonly coupled to WRF. In this study, the Noah LSM 2.7.1 version and the WRF-Hydro 3.0 version, as modified by Rummler et al. (2019), were used. WRF-Hydro, in comparison to the traditional 1-D LSM, enhances the physical description and mathematical resolution of surface and near surface hydrologic processes. It includes physics options for quasi 3-D saturated subsurface flow, 1-D or 2-D surface overland flow, 1-D channel routing, lake/reservoir routing, and baseflow processes. WRF-Hydro uses a disaggregation-aggregation procedure to resolve the hydrologic processes at a finer resolution than the LSM. Below, a brief description of the main modeled processes and characteristics is presented. For a detailed description of the model components the reader can refer to Gochis et al. (2015). A schematic representation of the model structure, as used in this study, is presented in Fig. 2.

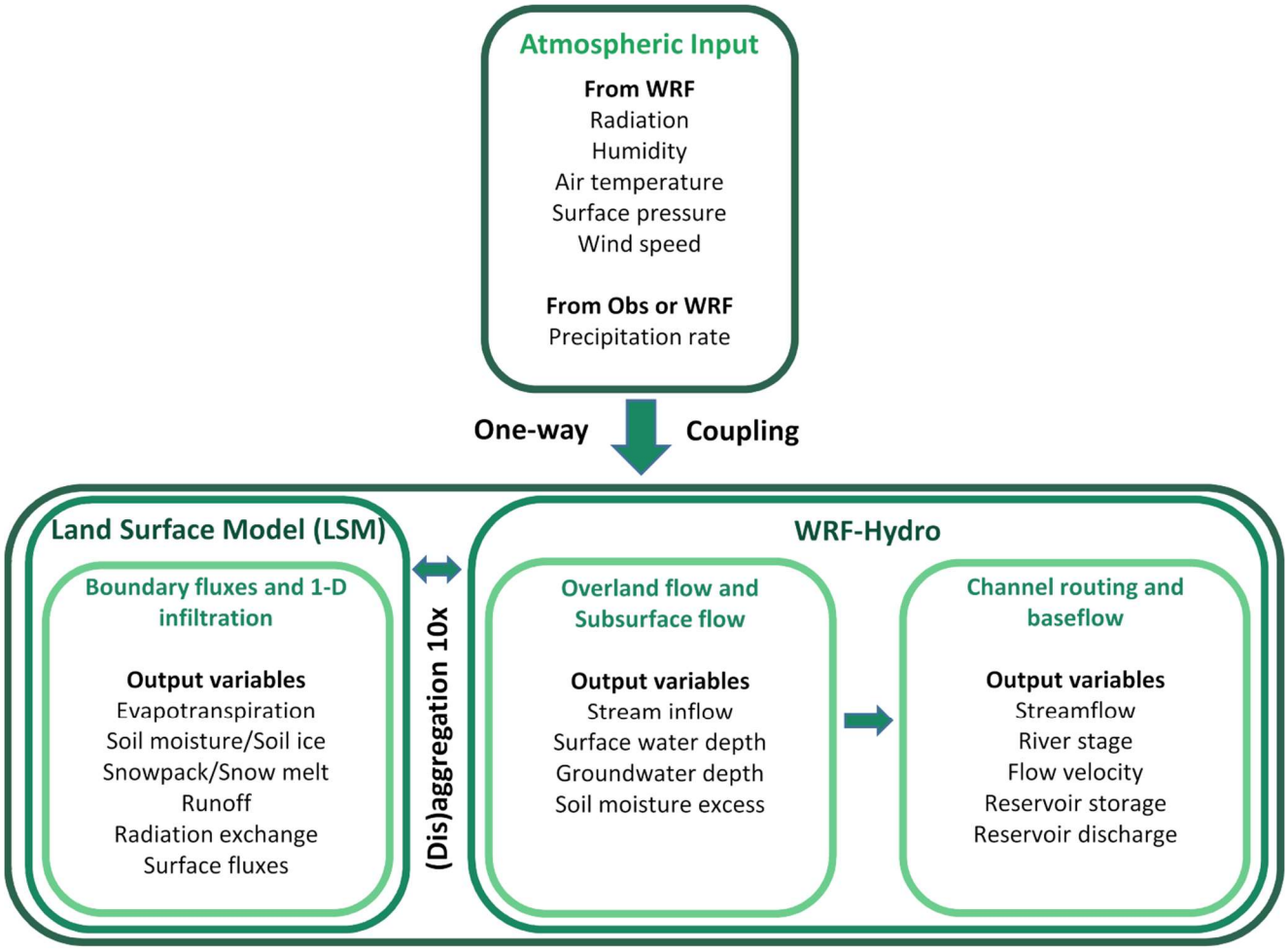

Figure 2. Schematic illustration of the model structure used in this study, including the coupling between WRF, the Noah Land Surface Model and WRF-Hydro routines (modified after Gochis et al., 2015).

One of the major advances of WRF-Hydro is the lateral subsurface flow component, which is calculated following the approach proposed by Wigmosta et al. (1994) and Wigmosta and Lettenmaier (1999). When precipitation reaches the surface, it can either infiltrate or run off. The partitioning between infiltration and runoff is controlled, besides the antecedent

soil moisture conditions, by soil properties. In the Noah-LSM, the infiltration capacity (DDT) is defined as a function of the soil moisture deficit (DD) and an exponential scaled adjustment (VAL), which is a function of the parameter KDT. It follows the approach of Schaake et al. (1996), with the difference that KDT is not directly calibrated but is expressed as a function of the saturated hydraulic conductivity and two scaling coefficients:

$$\mathrm{DDT} = \mathrm{DD} \cdot \mathrm{VAL}, \quad (3)$$

$$\mathrm{VAL} = \left(1 - e^{(-\mathrm{KDT}\cdot\mathrm{DT})}\right), \quad (4)$$

$$\mathrm{KDT} = \frac{\mathrm{REFKDT}\cdot \mathrm{K_{sat}}}{\mathrm{REFDK}}, \quad (5)$$

where DT is the time step duration [day]; K_{sat} [m s^{-1}] is the saturated hydraulic conductivity; REFDK is the reference (silty clay loam) saturated hydraulic conductivity (default 2E-06 m s^{-1}); and REFKDT is the infiltration partitioning scaling coefficient, which needs to be calibrated to empirically correct KDT for natural variability. As was demonstrated by previous studies (e.g., Naabil et al., 2017; Verri et al., 2017; Givati et al., 2016; Senatore et al., 2015), the model is sensitive to REFKDT. Once the water enters the soil, it moves vertically, through a four-layer soil column, until it reaches the saturated level and then laterally, according to the local gradient. In case the moisture content at the top of the soil column is larger than its water holding capacity (saturation), exfiltration occurs. The exfiltration amount is added to the infiltration excess and is routed over the surface. At the bottom of the soil column a vertical flux is calculated, using Richards equation (Richards, 1931). Drainage from the soil column is computed by multiplying the vertical flux with the SLOPE parameter, which can vary between 0-1, where 0 represents an impermeable boundary between the soil column and the underlying formations. The SLOPE parameter is assigned based on terrain slope classes through a table, however in an implicit way it expresses bedrock properties too (the higher the slope, the higher is the SLOPE coefficient in order to scale the projected map area over which deep drainage occurs). Drained water can be considered a loss or added to streamflow within the channel network through a conceptual baseflow module, if this is activated.

Regarding overland flow, WRF-Hydro allows water to pond on the earth's surface. A water retention depth is defined based on land use and vegetation cover. This parameter can be adjusted through a scaling factor (~~RETDEPRTFAC~~RTDPT), which can be specified for each model cell and can vary between 1-10 (Yucel et al., 2015). The fraction of ponded water exceeding the retention depth is available to overland flow routing. The routing is performed based on the diffusive wave formulation of Julien et al. (1995) and it can be resolved in both 1-D (Steepest Descent) or 2-D (x-y directions). Overland roughness is defined through the same tables as the retention depth and it can be adjusted through the overland-roughness routing factor (~~OVROUGHRTFAC~~OVRGH), which can vary between 0-1 (Yucel et al., 2015). Overland flow can re-infiltrate, evaporate or enter the channel network.

Water entering the channel network, which the user defines through a Digital Elevation Model, is routed based on a streamflow algorithm that uses an implicit, one-dimensional, variable time stepping diffusive wave formulation. Such formulation is a simplification of the St. Venant equations for shallow water flow. The algorithm does not allow overbank flow and therefore the 2-D modelling of floods (Rummler et al., 2019). Channels are considered trapezoidal in section. Their geometrical properties, including roughness, are defined based on stream order. These model parameters are entered through a table and they can be set by expert knowledge or adjusted during calibration. Along the channel network, reservoirs can be added. Water can flow into reservoirs through the channel network or when overland flow intersects them. Water can flow out of the reservoir through weir overflow and gate-controlled flow. These fluxes are governed by the reservoir parametrization (reservoir area, maximum water level in the reservoir, weir length, gate area, gate elevation, gate aperture coefficient). No exchanges occur between the reservoir, the atmosphere, and the soil column around the reservoir (i.e., evaporation and subsurface lateral flow from the reservoir are not accounted for).

When deep drainage from the soil column is not considered as a loss, WRF-hydro allows two mathematical simple solutions to account for baseflow. For both solutions, baseflow is calculated within sub-watersheds. The first solution consists of a simple pass-through model, meaning that the cumulated deep drainage occurring in a time step is equally redistributed to all

channel segments within the sub-watershed. The second solution consists of calculating a baseflow discharge [m^3 s^{-1}] (Q_{bf}) by means of an exponential bucket model, described by the following equation:

$$Q_{bf} = C \cdot \left(e^{a \cdot \frac{Z}{Z_{max}}} - 1 \right), \quad (6)$$

where C is the bucket coefficient [m^3 /s^{-1}], a is the bucket model exponent [-], Z_{max} is the maximum bucket level [m], and Z [m] is the bucket level at a certain time step. The user defines the C, a and Z_{max} parameters for each sub-watershed, together with a Z_{ini} [m] parameter to initialize the water storage in the bucket groundwater reservoir. At each time step the Z value is updated first adding the deep drainage contribution (*Perc*) and subsequently subtracting Q_{bf}:

$$Z_t = Z_{t-1} + \sum_{n=1}^{n=ncells} Perc_n - \frac{Q_{bf} \cdot DT \cdot 3600}{A}, \quad (7)$$

where A is the area of the sub-watershed [m^2], DT the model time step [day], n is the index for the sub-watershed cells, and ncells represents the number of cells of the sub-watershed. Similar to the first solution, Q_{bf} is equally redistributed to channel segments. If Z equals or exceeds Z_{max}, all deep drainage is transferred to the channel network.

4.2 WRF-Hydro model parameterization

The Noah LSM was parameterized over a 1 × 1 km^2 grid, while WRF-Hydro was run over a 100 × 100 m^2 grid. All simulations were performed in uncoupled mode, resolving the steepest descend formulation of the overland flow routine, with channel flow, baseflow and reservoir routines activated.

To run WRF-Hydro in uncoupled mode, the meteorological forcing needed are precipitation rate [mm s^{-1}], downward shortwave and longwave radiation [W m^{-2}], specific humidity [kg kg^{-1}], air temperature [K], surface pressure [Pa], near surface wind components [m s^{-1}]. For the calibration and validation runs, all variables except precipitation were taken from the WRF ERA-Interim downscaling experiments presented in (Zittis et al., (2017). These simulations incorporated the Grell-Freitas Ensemble Convection and the Ferrier Microphysics parameterization schemes, which were found to outperform the other tested configurations for the selected events. For precipitation, hourly observed gridded data were used (see Section 3.2 – Meteorological Data). For the simulation runs with WRF-modelled rainfall, all variables including precipitation were taken from the WRF experiments (Zittis et al., 2017). To derive soil moisture initial conditions, 15-day WRF spin-up runs were performed for both events. For Jan 89, the 15-day rainfall during spin-up was 99 mm and average soil moisture at the end of the simulation was 0.32 m^3 m^{-3}. The Nov-1994 event followed the dry summer and only a few scattered rain days occurred between the end of October and the beginning of November. The 15-day rainfall during spin-up was 18.4 mm and average soil moisture at the end of the simulation was 0.26 m^3 m^{-3}. Experimental data (Camera et al., 2018) show that in these conditions soil moisture for a gravelly sandy loam at 1300 m a.s.l. in the Troodos Mountains can vary between 0.10 and 0.15 m^3 m^{-3}. Therefore, the WRF-derived initial soil moisture values for November were halved.

Soil, lLand use and vegetation cover data were derived from the MODIS dataset through the WRF Pre-Processing System. According to the MODIS dataset, the Troodos Mountains has a uniform clay loam texture. However, field observations at higher elevation in the mountains, where the predominant lithologies consist of gabbro and ultramafic rocks, showed a gravelly sandy loam texture (Djuma et al., 2020; Camera et al., 2018; Cyprus Geological Survey Department, 1995). In addition, it is known that the Troodos gabbro is very weathered and therefore permeable (Christofi et al., 2020). Therefore, a sandy loam soil type was assigned to these areas. The related properties were attributed through the default table values implemented in WRF-Hydro (see Gochis et al., 2015). The hydrologic input layers (latitude, longitude, topography, flow direction, channel grid, lake grid, stream order, watersheds) were all calculated in ArcGIS® 10.2.2 starting from a 25 × 25 m^2 Digital Elevation Model (see Camera et al., 2017), resampled on the 100 × 100 m^2 grid, and the known locations of stream gauges and lakes. For the channel grid, a flow accumulation threshold of 1500 250 cells (2.5 km^2) was adopted.

For the definition of the deep drainage related parameter, two approaches were tested. First, Nnine slope terrain classes were derived following Silver et al. (2017) and SLOPE values were attributed accordingly. In the second case, for cells where the

bedrock consists of gabbro or ultramafic rocks (Cyprus Geological Survey Department, 1995), the slope terrain class (3) that maximizes drainage (representing a highly fractured system) was assigned. In both cases, ~~F~~for each slope terrain class, the related default SLOPE value listed in the WRF-hydro general parameters table was given. These changes in soil type and deep drainage based on geology affected mainly watersheds Ma, An, Pl, Ka, and At, ~~five are the only watersheds with~~ where 70% or more of the surface bedrock is made up of gabbro and ultramafic rocks (Table 1).. ~~The Troodos gabbro is very weathered and therefore permeable (Christofi et al., 2020).~~

Other general parameters are REFKDT~~,~~ and soil depth (SD), which were calibrated. REFDK~~, RETDEPRTFAC, and OVROUGHRTFAC~~ was~~ere~~ left to ~~their~~ its default value (2.00E-6 m s^{-1}). The WRF-Hydro parameter OVRGH was tested and values were assigned based on the sensitivity analysis, whereas RTDPT was kept constant all over the study area and a value of 1, consistent with a steep mountainous terrain, was assigned.

Channel geometrical parameters were attributed based on the study area knowledge of the authors (Table 2). ~~Default values were used for the Manning coefficients.~~ The initial channel water depth was set to the default value for dry conditions. Six reservoirs were characterized in the model setup (Table 3) according to data from the Cyprus Water Development Department (2009). At all reservoirs, outflow occurs for overflow only; the structures do not have a gate. Vyzakia reservoir was completed in early 1994, therefore it was not included in the Jan-1989 simulation.

Regarding baseflow, the parameter C was set equal to the long-term baseflow index, calculated from the 1980-2010 data series with the program PART (Rutledge, 1988). The initial level of the conceptual reservoir (Z_{ini}) was set as a fraction of the maximum level (Z_{max}), based on the saturation degree of the deepest soil layer at ~~time zero~~the end of the 15-day WRF spin-up period. The exponent a and Z_{max} were adjusted during calibration.

4.3 WRF-Hydro sensitivity analysis

A sensitivity analysis of the LSM parameters REFKDT, SLOPE, and soil depth (SD), which have been identified as sensitive parameters in previous studies (e.g., Fersch et al., 2019; Senatore et al., 2015), was performed for the Jan-1989 event. In addition, sensitivity runs for the OVRGH parameter and the saturated hydraulic conductivity (K_S) were performed, too. For these simulations, the baseflow routine was switched off. A reference scenario was set, with REFKDT and OVRGH equal to 1, ~~and~~ SD equal to 1.0 m, K_S equal to 2.45E-6 m s^{-1} (value attributed to clay loam soils in the soil parameter table), and the deep drainage parameter (SLOPE) assigned based on terrain slope, as in Silver et al. (2017). Parameters were changed one at a time. Eight values were tested for REFKDT (0.3, 0.5, 3.0, 5.0, 8.0, 10.0, 100.0, 1000.0), ~~and~~ two for SD (0.5 and 2.0 m), two for OVRGH (0.1, 0.5), three for K_S (3.38E-6 m s^{-1} as for loam, 5.23E-6 m s^{-1} as for sandy loam, 1.41E-5 m s^{-1} as for loamy sand), and a different set of SLOPE values was assigned based on terrain slope and geology. Also, to demonstrate the equifinality of calibrating REFDK and REFKDT, as suggested by eq. 5, two extra runs were performed for REFDK values of 4.00E-6 m s^{-1} and 6.67E-7 m s^{-1}.The relative sensitivity (S) was computed according to the following formula:

$$S = -\frac{(Vtot_i - Vto_{ref})}{Vtot_{ref}}, \quad (\text{~~7~~8})$$

where $Vtot$ is the total volume discharged during the simulation period, ref refers to the reference scenario, and i to the perturbed value.

Table 2. WRF-Hydro channel parameter values used in this study (*Bw* is the channel bottom width, *HLINK* is the initial depth of water in the channel, *ChSSlp* is the channel side slope, and *MannN* is the Manning's roughness coefficient).

Stream Order	*Bw* [m]	*HLINK* [m]	*ChSSlp* [-]	*MannN* [-]
1	1.5	0.02	3.00	0.14
2	3.0	0.02	1.00	0.12
3	5.0	0.02	0.50	0.09
4	10.0	0.03	0.18	0.09

Table 3. Characteristics of the reservoirs included in the WRF-Hydro simulations; Long and Lat are longitude and latitude, respectively.

Watershed	Reservoir Name	Long [deg]	Lat [deg]	Reservoir Area [m^2]	Reservoir max elevation [m a.s.l.]	Reservoir ave elevation [m a.s.l.]	Weir length [m]
Vyzakia	Xyliatos	33.038	35.006	80000	537.5	529.9	15.0
Vyzakia	Vyzakia	33.029	33.029	160000	353.8	319.0	6.0
Akaki	Palaichori	33.130	34.928	110000	719.6	704.5	9.8
Akaki	Kalochorio	33.155	34.981	13000	533.5	528.5	22.5
Kotsiatis	Lythrodontas-1	33.274	34.944	10000	460.3	455.3	19.0
Kotsiatis	Lythrodontas-2	33.288	34.949	15000	422.5	413.5	33.8

4.4 WRF-Hydro calibration and validation with observed precipitation

Calibration runs were evaluated for each watershed against Jan 1989 daily observed streamflow, based on five performance indices. The selected set of indices contains both absolute error and goodness-of-fit measures, as suggested by Legates and McCabe (1999). They are percent ~~BIAS~~bias *(PBIAS),* Mean Absolute Error (*MAE*), Nash-Sutcliffe Efficiency (*NSE* - Nash and Sutcliffe, 1970), modified Nash-Sutcliffe Efficiency (*mNSE*, Krause et al., 2005), and Kling-Gupta Efficiency (*KGE*, Kling et al., 2012).

Soil Depth is constant throughout the domain, therefore it was fixed at the value that returned the best performance indices in the majority of the watersheds, following an evaluation of the sensitivity analysis runs. Similarly, SLOPE parameters were assigned using the slope terrain class map allowing the best performance during sensitivity. ~~Calibration focused on three parameters, REFKDT and two baseflow bucket parameters (α and Z_{max})~~. REFKDT and OVRGH ~~was~~ were initialized, in each watershed, based on the evaluation of the sensitivity runs through performance indices, as for SD. For the baseflow bucket routine, initial values of α and Z_{max} ~~parameters~~ were set to the default. Next, ~~REFKDT, α and Z_{max}~~the initialized parameters were fine-tuned based on a trial and error procedure for all watersheds. Modifications were applied to a single parameter at the time and if changes could not improve the model performance according to three indices out of five after five attempts, the parameters were retained. Commonly applied changes were ±1 for REFKDT, ±0.1 for OVRGH, ±0.5 for α, and ±10% of the actual value for Z_{max}. Smaller (larger) changes were applied only in watersheds where the response of streamflow was (not) particularly sensitive to specific parameters. The parameterization of Z_{max} was aimed at filling the reservoir after the rainfall peak, between 10 January at midnight and 11 January at noon, to simulate the observed recession of the hydrograph. For those watersheds that highly overestimated the baseflow due to spilling out of the groundwater reservoir, Z_{max} was further increased. A good fit between observed and simulated flow before the peak was the target for the calibration of the exponent α. The calibrated model was subsequently applied to the Nov-1994 event for validation. The same five model performance indices were used for the evaluation.

4.5 WRF-Hydro simulations with WRF-modelled precipitation

The WRF-modelled precipitation (Zittis et al., 2017) was averaged over each of the 22 watersheds and the daily values were compared to observed data by means of *BIAS*, *MAE* and *NSE*. To evaluate how deviations from the observed rainfall pattern affected the hydrologic model performance in these small mountain watersheds, the calibrated version of WRF-Hydro model was run with the WRF-modelled hourly precipitation forcing. Modelled streamflow was evaluated with observed data, similar as in the calibration phase.

4.6 WRF-Hydro evaluation with observed and modeled precipitation at hourly scale

For watersheds presenting daily *NSE* equal to or larger than 0.50 for both the calibration and the validation event, model performance was also investigated at hourly resolution. The *NSE*, *KGE* and *MAE* were computed for the hourly streamflow values simulated with both observed and modeled precipitation.

5 Results and discussion

5.1 Sensitivity analysis

The results of the sensitivity analysis are presented in Fig. 3 as boxplots. Each boxplot represents the sensitivity of the modelled total discharge volume, over the 22 watersheds, for the perturbation applied, in comparison to the reference simulation. The boxplots show that in the suggested calibration range (0.5-5.0, Gochis et al., 2015) REFKDT is very sensitive. Although the sensitivity decreases for REFKDT values larger than 5.0, variations in the discharged volume can be observed up to REFKDT values equal to 100.0. Further increases in REFKDT (see REFKDT 1000.0) do not cause any variations in discharge, suggesting that the model already infiltrates at its maximum capacity. The variability over the watersheds is related to ~~both infiltration processes (soil moisture conditions and texture controlling the hydraulic conductivity) and overland flow processes (controlled by local topography, land use and vegetation)~~local conditions (e.g., soil moisture distribution, area, topography, type of vegetation). Precipitation, which is not homogeneous throughout the study area, can play a role in causing different responses as well.

The two simulations ran with REFDK values of 4.00E-06 m s^{-1} and 6.67E-7 m s^{-1} returned discharged volumes equal to those obtained with REFKDT values of 0.5 and 3.0, respectively. These results confirm the equifinality of the two parameters and make it clear that REFDK calibration should be avoided. As shown in Eq (3-5), REFDK automatically adjusts the infiltration capacity for the effect of soil texture, whereas any other effects on the partitioning of rainfall into surface runoff and infiltration can and should be calibrated through REFKDT.

The sensitivity analysis shows also an important role played by Soil Depth. Especially in mountainous areas, soils are usually thin. This limited soil thickness affects the total amount of water retained by the soil, favoring a partitioning of the available water between infiltration and surface runoff towards the latter. Similar observations are reported by Fersch et al. (2019), while commenting the offset between modelled and observed soil moisture content in mountainous catchments in Bavaria (Germany). To overcome the issue, in other land surface models (e.g., Brunke et al., 2016) variable soil thickness has been implemented and tested.

Regarding OVRGH, results show that it has a slight control on the total volume discharge, as also presented in Yucel et al. (2015), while it has almost no effect on delaying the peak (Fig. 4). More sensitive than OVRGH is Ks, suggesting a possible important impact of the soil type and property definitions on the model output. Senatore et al. (2015) presented one of the few WRF-Hydro studies that calibrated a hydraulic conductivity related parameter, although they focused on the saturated soil lateral conductivity. SLOPE appeared to have a low sensitivity, although in the mountain watersheds, where it changed, a small reduction in the total discharged volume was observed.

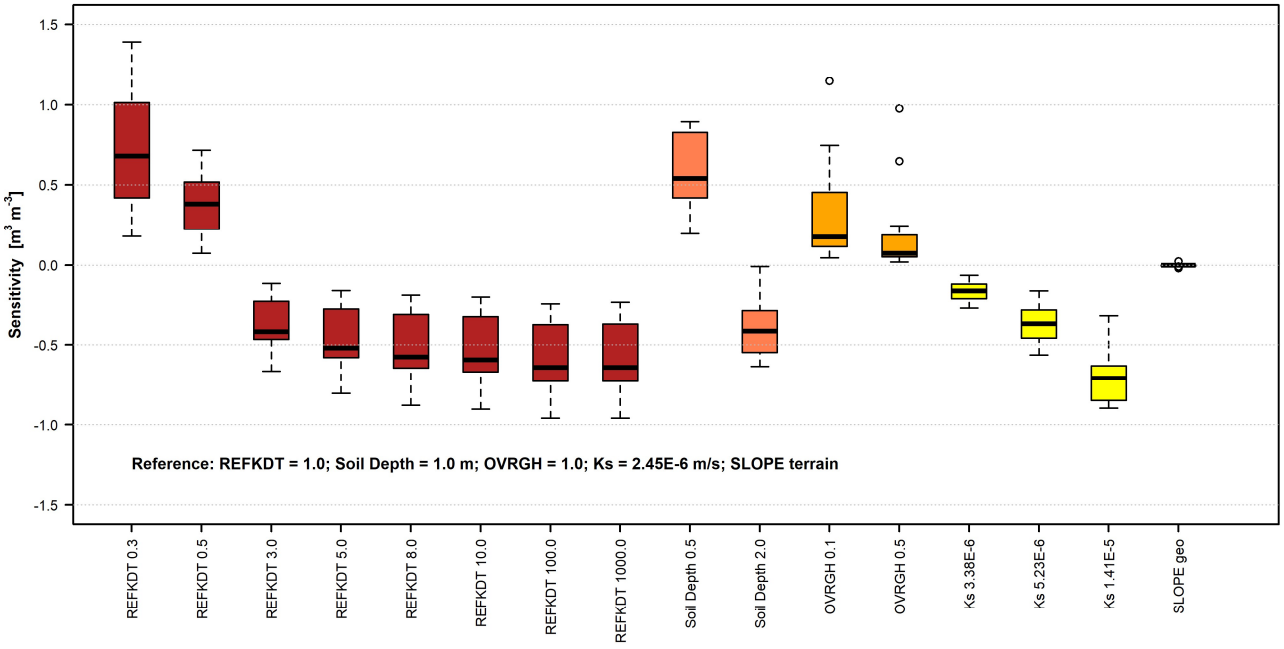

Figure 3. Boxplots of the sensitivity of the modelled streamflow to perturbations (x-axis) in REFKDT (infiltration partitioning scaling coefficient), ~~and~~ Soil Depth, OVRGH (overland roughness factor), Ks (saturated hydraulic conductivity), and SLOPE geo (deep drainage parameter defined based on slope terrain and geology) relative to a defined reference scenario (SLOPE terrain represents the slope parameter defined based on slope terrain only, as in Silver et al., 2017).

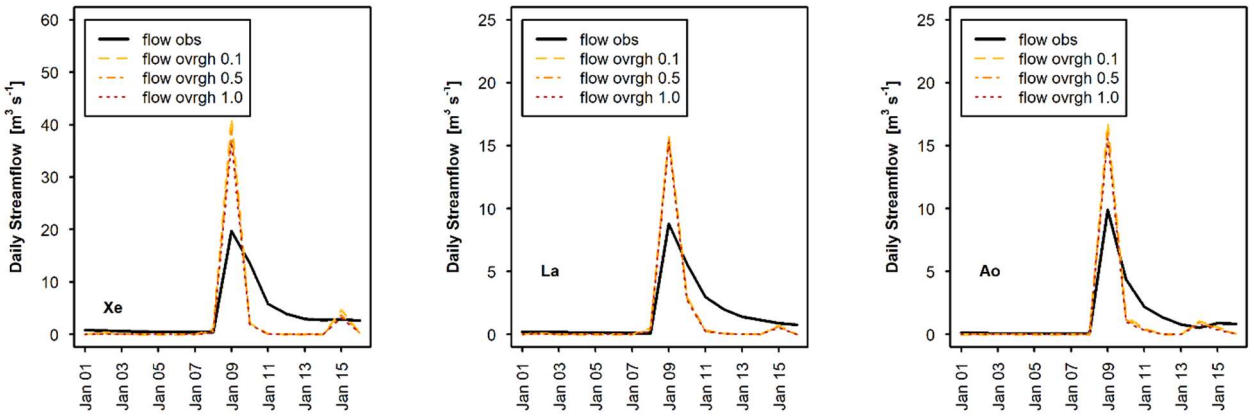

Figure 4. Hydrographs obtained at three different watersheds for OVRGH values of 0.1 (flow ovrgh 0.1), 0.5 (flow ovrgh 0.5), and 1.0 (flow ovrgh 1.0), in comparison to observed flow (flow obs). For watershed short names refer to Table 1.

360

5.2 WRF-Hydro calibration and validation with observed precipitation

The calibrated parameters are listed in Table 4. Soil depth was set equal to 1 m for all watersheds, because it was the value returning the best performance indices (Fig. 4) in 16 out of 22 catchments (average *NSE* improvement equal to 0.14). SLOPE attributed based on both terrain slope and geology resulted in slightly better performance indices in the mountain watersheds 365 than SLOPE attributed through terrain slope only. Therefore, it was selected for the final parameterization. Also, for all watersheds OVRGH was set equal to 1 because it was the value returning the best performance indices in 19 out of 22 watersheds. Furthermore, considering that OVRGH effects total discharge volume and not hydrograph shape, its calibration would have been equifinal to REFKDT. ~~Fourteen~~ Twelve watersheds have a REFKDT coefficient larger than 5.0, which is outside the 0.5-5.0 range suggested by Gochis et al. (2015), but none has a REFKDT lower than 0.5. The hydrographs of all 370 watersheds are shown in the supplementary material. Fig. S1 and Fig. S2 show hydrographs, including the baseflow component, related to responses to observed rainfall for the Jan-1989 event and the Nov-1994 event, respectively.

Table 4. Calibrated parameters (REFKDT, infiltration partitioning scaling coefficient; *C*, baseflow bucket coefficient; *α*, bucket exponent; Z_{max}, maximum bucket level) for the 22 watersheds with their maximum (MaxQ) and average (AveQ) discharges for the two analyzed events; for watershed short names refer to Table 1.

Watershed short name	Max Q89 [$m^3 s^{-1}$]	Ave Q89 [$m^3 s^{-1}$]	Max Q94 [$m^3 s^{-1}$]	Ave Q94 [$m^3 s^{-1}$]	REFKDT [-]	*C* [$m^3 s^{-1}$]	*α* [-]	Z_{max} [m]
Xe	19.7	3.7	8.2	1.1	5.0	0.30	2.0	30.0
Af	4.1	1.0	1.1	0.2	50.0	0.09	0.7	150.0
St	12.5	2.7	4.1	0.6	2.5	0.20	2.4	100.0
Ar	3.2	1.0	1.5	0.2	12.0	0.08	2.6	70.0
Pg	1.1	0.3	0.3	0.1	7.0	0.04	1.1	3.30.5
Le	3.3	0.9	1.4	0.3	1.82.0	0.07	2.22.0	1.51.4
Mk	0.3	0.1	0.1	0.0	8.0	0.01	3.2	20.010.0
Py	4.1	1.4	2.2	0.4	5.0	0.15	1.4	200.0
Li	12.3	3.0	5.4	1.0	7.0	0.27	1.2	72.070.0
Ma	3.7	1.2	2.9	0.6	50.0100.0	0.19	1.21.6	600.0100.0
An	1.8	0.7	3.3	0.8	50.0100.0	0.24	1.6	600.0100.0
Pl	1.3	0.4	1.9	0.3	50.0100.0	0.05	0.82.1	600.0130.0
Ka	9.2	2.6	10.5	1.9	50.0100.0	0.30	1.61.2	500.0130.0
At	2.9	1.0	1.9	0.5	10.0100.0	0.04	0.82.1	220.060.0
La	8.8	1.6	6.4	0.9	6.08.0	0.05	2.3	53.015.0
Vy	15.9	3.5	12.0	2.4	6.04.0	0.09	3.02.6	12.050.0
Pe	58.0	7.5	35.0	5.9	1.0	0.29	2.5	8.0
Ak	49.0	7.7	28.0	5.7	0.8	0.20	3.01.4	5.0
Ao	9.9	1.4	5.3	1.1	3.0	0.03	2.1	10.0
Pd	26.0	3.2	8.9	1.9	2.0	0.07	2.2	10.0
Ko	18.0	3.6	15.0	3.0	6.05.0	0.05	3.53.2	2.42.0
Ni	18.2	4.1	16.5	3.0	7.0	0.05	2.63.2	3.0

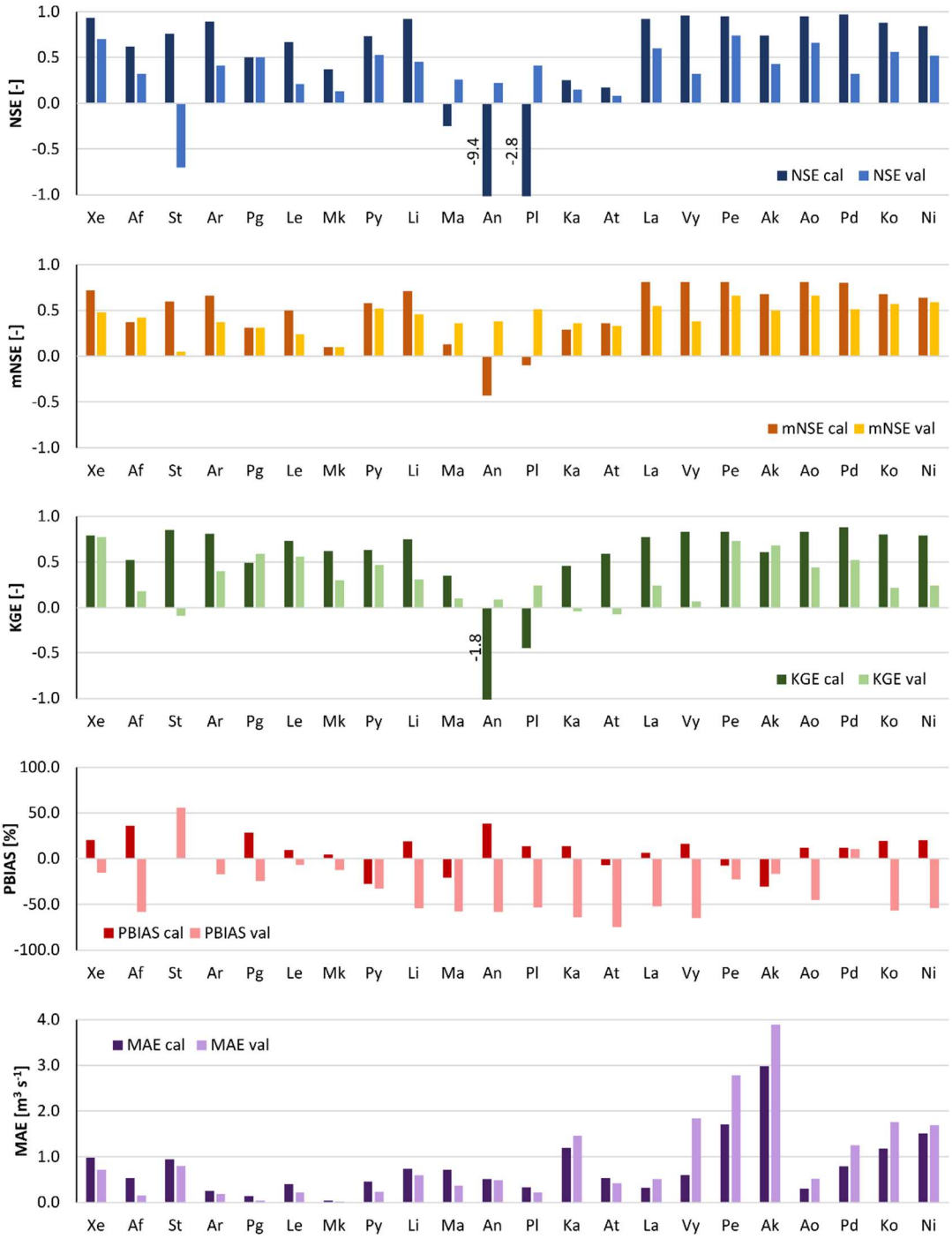

Figure 5. Performance indices (NSE, Nash-Sutcliffe Efficiency; mNSE, modified Nash-Sutcliffe Efficiency; KGE, Kling-Gupta Efficiency; BIAS; MAE, Mean Absolute Error) calculated on daily streamflow resulting from observed rainfall for the 22 watersheds using the calibrated set of parameters for both Jan 1989 (cal) and Nov 1994 (val). For watershed short names refer to Table 1.

The parameterization of watersheds Ma, An, Pl, Ka, and At is peculiar. These watersheds are mainly characterized by sandy loam texture (i.e., higher Ks than the other watersheds), maximum deep drainage obtained by using the SLOPE parameters based on slope terrain and geology, ~~because even with~~ very high REFKDT values, and very large groundwater storage. However, ~~no reasonable~~poor model fit indices (for some watersheds even negative) ~~could be~~were obtained for the calibration period (Fig. 54). Conversely, the same watersheds show positive *NSE* values and negative *PBIAS* (i.e., slight underestimation of the peak discharge), for the validation event. Overestimation of runoff in Jan 1989 could have been related to the modeling of snow and snowmelt in the LSM. Both observed and modeled temperature values for ~~This is probably due to the fact that~~ the upstream areas of these watersheds showed negative values, indicating that ~~are located at the highest elevation and that~~ part of the precipitation ~~during the calibration~~ was snow ~~rather than rainfall.~~, ~~which is not explicitly considered in~~

~~the model~~. ~~-~~In Fig. 6~~5~~, the comparison between the observed and simulated daily hydrographs for the Jan-1989 event is shown. The subdued response of the streamflow to the extreme precipitation is clear for watershed Pl, which is considered representative of the behavior of all five watersheds mentioned above, and it is clear that the simulated hydrograph overestimates the observed peak flow of the event. ~~According to the MODIS soil map used, the soil type is uniform (clay loam) over the study area. However, geological differences between these five watersheds and the other watersheds are evident in Table 1. These five are the only watersheds with 70% or more of the surface bedrock made up of gabbro and ultramafic rocks. The Troodos gabbro is very weathered and therefore permeable (Christofi et al., 2020). Improvements could have been obtained by using a more detailed soil map (e.g., Camera et al., 2017), possibly leading to an increase in the saturated hydraulic conductivity of the soil and an increase in drainage to the bedrock. Also, d~~Different bottom boundary conditions and snow processes modelling, as those implemented in the Noah Multi-Physics LSM, could improve the simulation results.

Overall, in all other watersheds the model behaves satisfactorily, with goodness-of-fit scores (*NSE*, *mNSE* and *KGE*, Fig. 4~~5~~) usually higher than 0.5 for the calibration run and larger than 0.0 for the validation event. Exceptions are watershed Mk for the calibration run and watershed St for the validation run. Looking at the hydrographs (Fig. 6~~5~~ and Fig. 7~~6~~), it is observed that Mk presents a very low discharge due to its limited area (Table 4). Therefore, small biases between observed and modelled streamflow produce poor goodness-of-fit indices. Also, Mk is the only watershed showing higher rainfall and flow peaks towards the end of the Jan-1989 event rather than in the middle. The model slightly underestimates the flow peak occurred on January 9th and overestimates the flow at the end of the simulation period. For St, the ~~observed discharges show a two-day peak, while the model concentrates the discharge in the first day only,~~model reacts sharply to precipitation input, simulating well the flow peak occurred on January 9th but overestimating the flow at end of the simulation period of the Jan-1989 event and above all the peak of the Nov-1994 event, therefore affecting the performance scores.

In the eastern part of the modelling domain (La to Ni), for the calibration event both initial baseflow and the discharge peak are well modelled in all watersheds (Fig. 6~~5~~). Differences between observed and simulated hydrographs can be observed in the post-peak, ~~especially~~ for watersheds ~~Pe (not shown) and~~ Ak, Pe (Fig. S1), Ko and Ni. ~~Both~~ Ak and Pe ~~watersheds~~ present a very high peak flow (> 50 $m^3 s^{-1}$) and an underestimation of the ~~baseflow~~ receding limb of the hydrograph in the following days, which causes the ~~high~~ negative *PBIAS* and high *MAE* values visible in Fig 5~~4~~. In the case of Ko and Ni, the receding limb shows a little overestimation. For the validation event (Fig. 7~~6~~), the peak is well simulated in ~~Ak~~ Pe and Ao, ~~-~~ slightly overestimated in Ak and Pd, underestimated in La, Vy, Ko, and Ni (~~and in~~ Pe and Pd, ~~not shown~~Fig. S2). In the post peak phase, ~~but~~ the simulated hydrographs show negative biases in comparison to the observed ones~~, in the post-peak phase~~in all watersheds~~, as for Jan 1989~~. As it is visible in Fig S1 and Fig S2, flow in the receding limb of the hydrograph is mainly made up of baseflow. For Jan-1989 event, in all these watersheds the groundwater reservoir is filled up on January 10th and baseflow consists of the water spilling out from it. This water volume, redistributed along the channel network, is generally able to reproduce the hydrograph shape, except in Ak. In Nov 1994, no groundwater spilling is observed during the simulation and the receding limb is underestimated. Therefore, this could be partly due to a non-perfect reproduction of the model initial conditions and partly related to an underestimation of interflow and baseflow.

5.3 WRF-Hydro simulations with modeled precipitation

Figure 8~~7~~ presents the performance indices of the WRF-modelled rainfall. Fig. S3 and Fig. S4 (in the supplementary material) show hydrographs, including the baseflow component, related to responses to modelled rainfall for all watersheds for the Jan-1989 event and the Nov-1994 event, respectively. The modelled rainfall is generally closer to observations for the Jan-1989 event than for the Nov-1994 event, as testified by the higher *NSE* (except for Le) and lower *MAE* values (Fig. 8~~7~~). As can be seen in Fig. 6~~5~~, the Jan-1989 event appears as a single day of intense precipitation, followed by a few scattered

low rainfall days that can show a moderate intensity towards the end of the simulation period. During Jan-1989, WRF-modelled rainfall is usually able to fit the observed daily precipitation trend over all watersheds, with slight variations in the calculated daily amounts as suggested by the generally low bias (Fig. 87). In percentage, over the 22 watersheds rainfall *PBIAS* ~~vary~~ varies between -35% and ~~50~~53%, with an average of absolute values equal to 17%. Average *NSE* and *MAE* of the WRF-modelled rainfall~~, calculated over the daily averages of these 16 watersheds,~~ are 0.83 and ~~4.2~~4.5 mm d^{-1}, respectively.

Figure 7 shows that the Nov-1994 event is constituted of two days of moderately low precipitation, followed by three days of intense precipitation. The simulated event shows higher rainfall amounts in the preceding days and a loss of intensity after the first of the three high precipitation days. Over the 22 watersheds, average *NSE*, absolute *PBIAS*, and *MAE* are 0.48, 20%, and 8.9 mm d^{-1}, respectively.

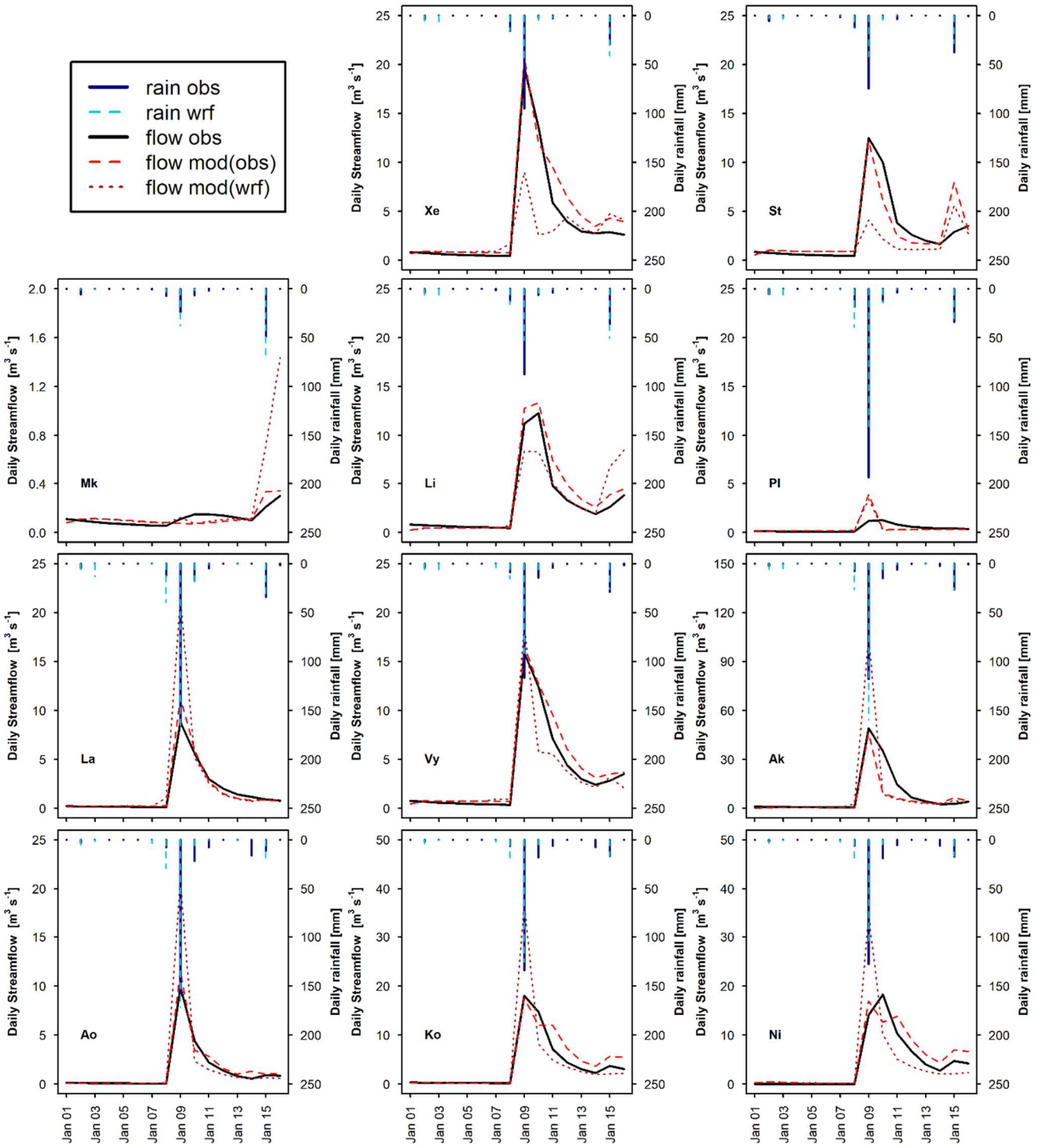

Figure 6. Observed daily hydrographs (flow obs) and hydrographs obtained with the calibrated WRF-Hydro model (flow mod) forced with observed rainfall (rain obs) and with WRF modelled rainfall (rain wrf) for the Jan-1989 calibration event, for 11 representative watersheds (see Table 1 for watershed short names).

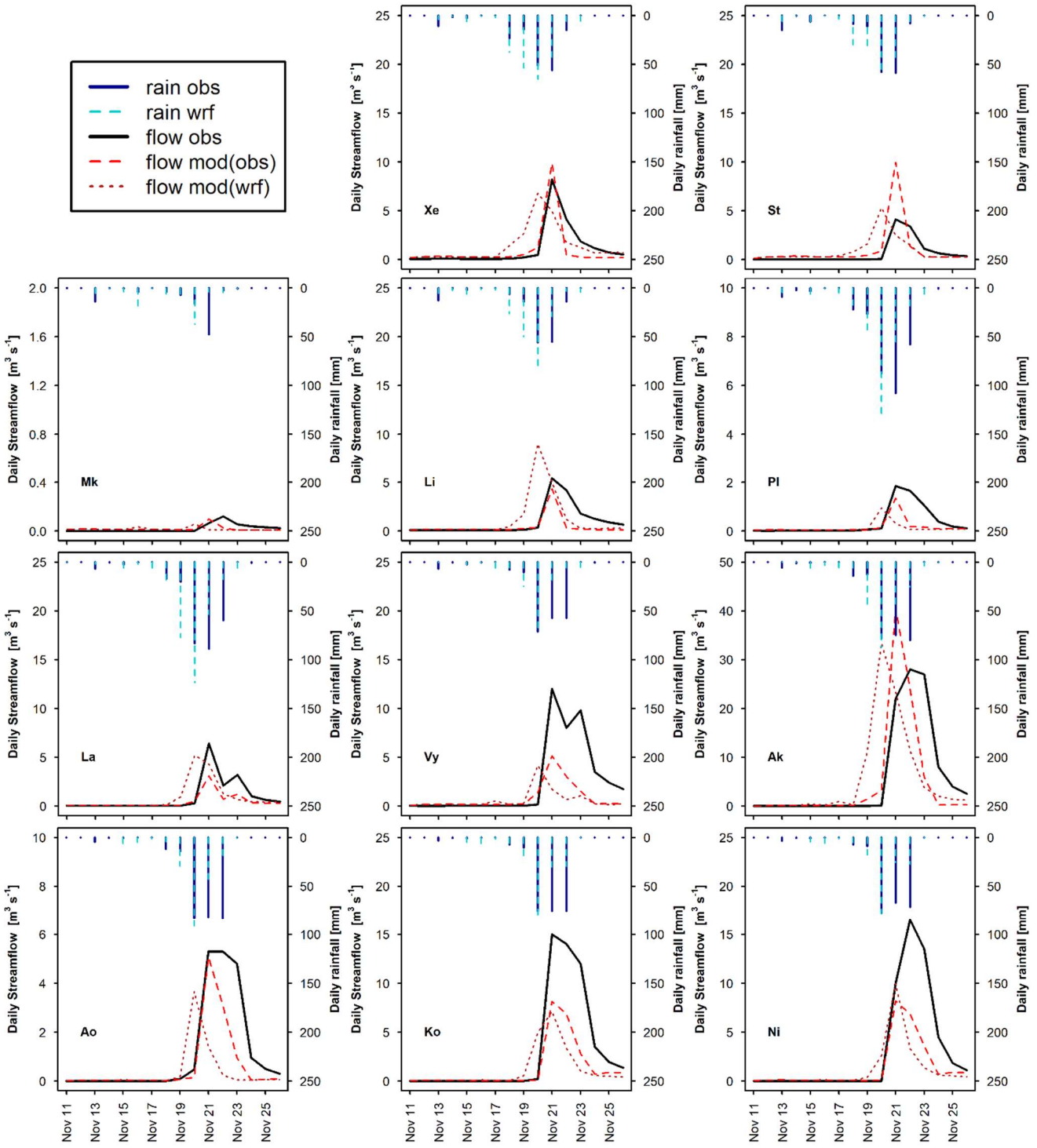

445

Figure 7. Observed daily hydrographs (flow obs) and hydrographs obtained with the calibrated WRF-Hydro model (flow mod) forced with observed rainfall (rain obs) and with WRF modelled rainfall (rain wrf) for the Nov-1994 validation event, for 11 representative watersheds (see Table 1 for watershed short names).

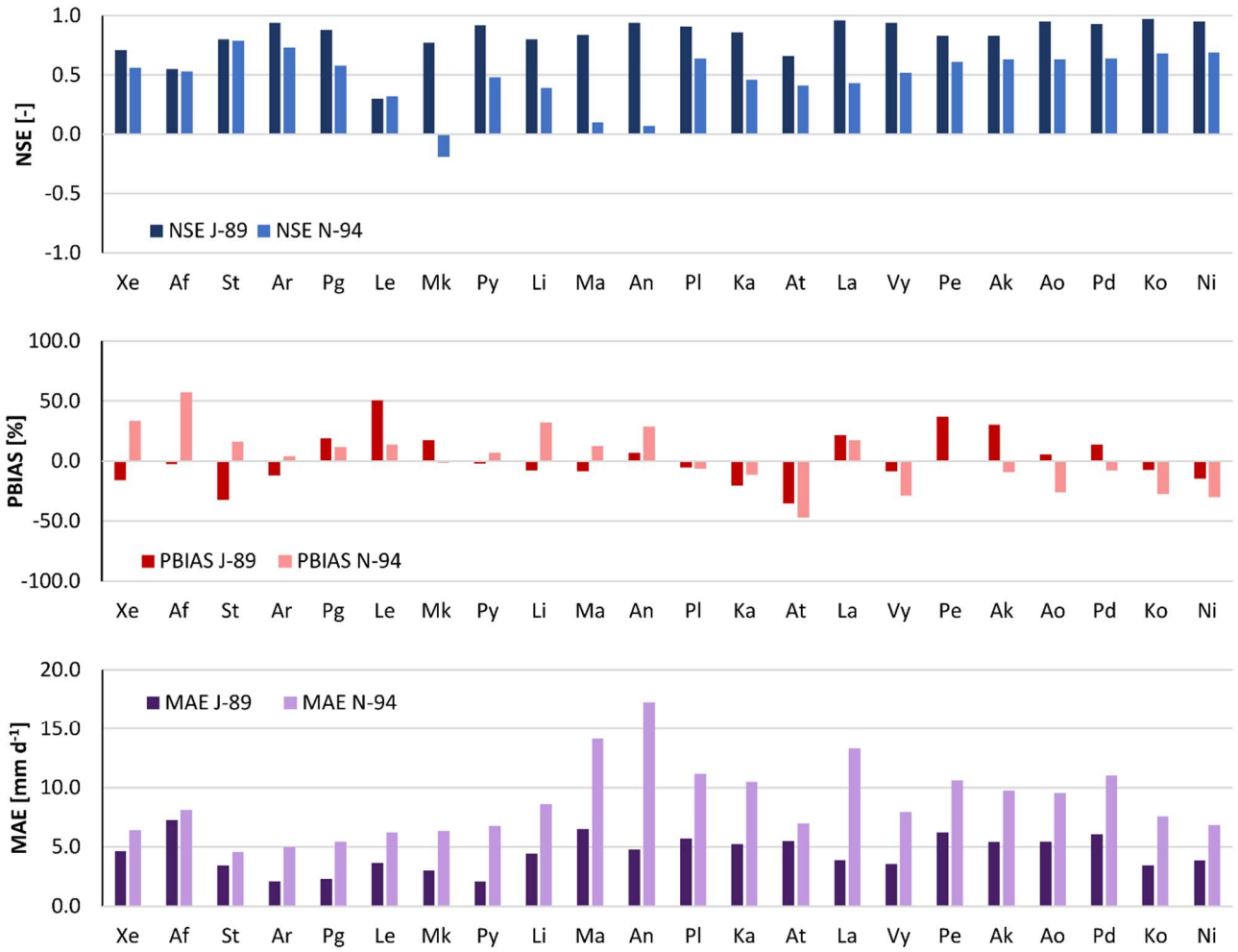

Figure 8. Performance indices (NSE, Nash-Sutcliffe Efficiency; BIAS; MAE, Mean Absolute Error) of daily WRF-modelled rainfall over the 22 watersheds both Jan 1989 (J-89) and Nov 1994 (N-94) events. For watershed short names refer to Table 1.

The modelled rainfall in Jan 1989 results in hydrograph shapes similar to the observed ones but still in goodness-of-fit indices that are often negative. With observed rainfall forcing, the simulated daily hydrograph returned negative *NSE, mNSE and KGE* values (Fig. 5) in ~~six~~three, ~~five~~ two and ~~five~~ two watersheds, respectively. With WRF-modelled rainfall forcing the number of watersheds with negative indices (Fig. 9) increases up to ~~thirteen~~twelve, ~~eight~~six, and ~~ten~~nine, respectively. ~~Passing~~ Moving from observed to WRF-modelled rainfall, both streamflow *NSE* and *MAE* indicate a loss in model performance in all watersheds except ~~four~~ three (Ma, Pl, Ka~~, At~~), which are those characterized by very negative goodness-of-fit indices in the calibration run. The average streamflow *MAE* ~~increased by 1.09 m^3 s^{-1}, corresponding to 93%~~almost doubled, and ranged between 0.~~12~~ 09 m^3 s^{-1} in ~~Py~~ Mk and ~~4.55~~3.89 m^3 s^{-1} in Pe. ~~These large errors were caused by relatively small errors in the WRF-modelled precipitation. Average *NSE* and *MAE* of the WRF-modelled rainfall, calculated over the daily averages of these 16 watersheds, are 0.83 and 4.2 mm d^{-1}, respectively.~~ The absolute value of flow *PBIAS* decreased in ~~eight~~ seven watersheds (Af, Li, ~~Ma,~~ Pl, ~~Ka~~Vy, Ak, Ko, Ni) but on average increased by ~~8.6~~21.5% ~~times~~ (~~58~~ 96.6% in Pg and 120.3%~~times~~ in Le ~~and 110 times in St~~).

~~Figure 6 shows that the Nov 1994 event is constituted of two days of moderately low precipitation, followed by three days of intense precipitation. The simulated event shows higher rainfall amounts in the preceding days and a loss of intensity after the first of the three high precipitation days.~~ Regarding streamflow for Nov-1994 event~~Consequently~~, the peak discharge is simulated to occur one day earlier than observed in most watersheds. This caused negative streamflow performance indices in eighteen watersheds for *NSE*, in eight watersheds for *mNSE*, and in ~~ten~~ eleven watersheds for *KGE* (Fig. 9), while with the forcing of observed rainfall negative indices were found in one, zero, and ~~two~~ three watersheds, respectively (Fig. 5).

These results indicate that a small shift in time or space of modelled rainfall, in comparison to observed precipitation, can strongly modify the hydrologic response of small watersheds to extreme events. This is particularly evident in watersheds Pg and Mk, which are among the smallest and those characterized by the lowest average discharge in both events (Fig. 6, Fig. 7, Fig. S3, Fig. S4). Although their rainfall performance indices (Fig. 8) do not show particularly large errors (except a negative NSE for Mk in Nov 1994), streamflow fit indices present very negative values and streamflow PBIAS is very high as well (Fig. 9).–The implementation of rainfall data correction or assimilation schemes could improve the forecasts of the atmospheric-hydrologic modelling chain, as demonstrated and discussed by previous studies (e.g., Avolio et al., 2019; Verri et al., 2017; Yucel et al., 2015). Recently, increasing efforts have been made to implement two-way coupled modelling systems, which were found to improve the overall skills of the modelling system (e.g., Senatore et al., 2015). However, the hydrologic component calibration is still usually performed based on observed precipitation data (e.g. Fersch et al., 2019; Givati et al., 2016).

The rainfall fields modelled by Zittis et al. (2017) and used in this study were downscaled from the ERA-Interim re-analysis dataset. The decision to use these modelled data was driven by the fact that ERA-Interim presents a resolution closer to that of existing forecasting, decadal prediction, and global climate models, therefore it resembles a modelling chain for forecasting applications and climate change projections (e.g., Reyers et al., 2019; Saha et al., 2014). For future studies ERA5, thanks to its finer resolution and the availability of ensemble members for uncertainty estimates, will be a valuable data source for improving the modelling chain over small (< 100 km^2) catchments.

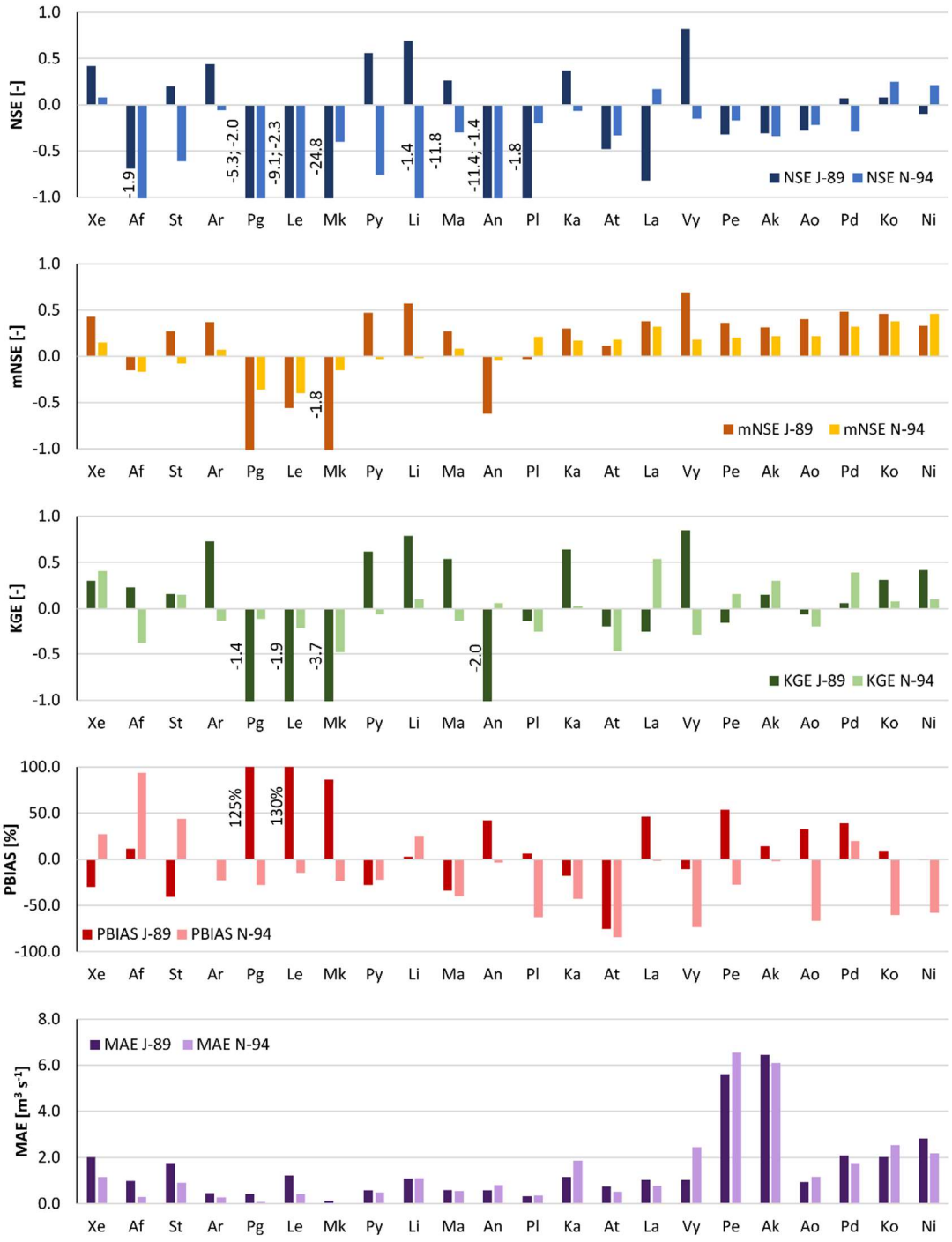

Figure 9. Performance indices (NSE, Nash-Sutcliffe Efficiency; mNSE, modified Nash-Sutcliffe Efficiency; KGE, Kling-Gupta Efficiency; BIAS; MAE, Mean Absolute Error) calculated on daily streamflow resulting from WRF-modelled rainfall for the 22 watersheds using the calibrated set of parameters for both Jan 1989 (J-89) and Nov 1994 (N-94) events. For watershed short names refer to Table 1.

5.4 WRF-Hydro with observed and modeled precipitation evaluation at hourly scale

Figure 10 shows the comparison between observed and modelled hourly hydrographs for three out of the ~~six~~ seven watersheds that had modelled daily streamflow *NSE* larger than 0.5 in both calibration and validation events. The ~~two~~ four watersheds that are not shown are Pg (hourly streamflow data not available), Pe, ~~and~~ Ko, and Ni (rating curve not available for peak flow). Looking at the streamflow modelled with observed rainfall as forcing, hourly peaks are generally overestimated and the modelled streamflow response to rainfall appears more immediate (pulse-like) than the observed streamflow. The overestimation is more evident for the Nov-1994 validation event than for the Jan-1989 calibration event. In

addition, ~~baseflow~~ the receding hydrograph is well modelled for the calibration event but not so well for the validation event. This result is similar to what was observed for daily streamflow and was attributed to the possible non-perfect reproduction of the model initial conditions and underestimation of interflow. The ~~decent baseflow~~ fairly good post-peak simulations lead to reasonable hourly performance indices for the Jan-1989 event. However, even with an *NSE* of 0.80 and a *KGE* of 0.72 for watershed Ao, the 17.9 $m^3 s^{-1}$ hourly peak flow was overestimated by 18%.

The response of hourly streamflow to WRF-modelled rainfall shows similar behavior. The shape of the hydrographs is defined by rainfall pulses, in terms of both time of response and size of peaks. Even more than for daily outputs, it is evident that small differences in rainfall distribution and amount can cause large differences between observed and modelled streamflow (see performance indices).

A possible improvement may be obtained by an increase in channel ~~and overland~~ roughness coefficients. This would allow slower flow, ~~higher infiltration,~~ and a smoothing of the peaks. Especially in dry Mediterranean areas, characterized by streams with seasonal flow, the vegetation (and consequently the roughness conditions) can be very different at the end of the dry period (vegetation grown within the stream, dry understories and bushes and bare cropland overland) and in the middle of wet winter (water within the riverbed, green vegetation cover overland). This could be described with the inclusion of a seasonal variation of channel and overland roughness coefficients in the model. However, rainfall data with high spatial and temporal resolution would be essential to test this model modification.

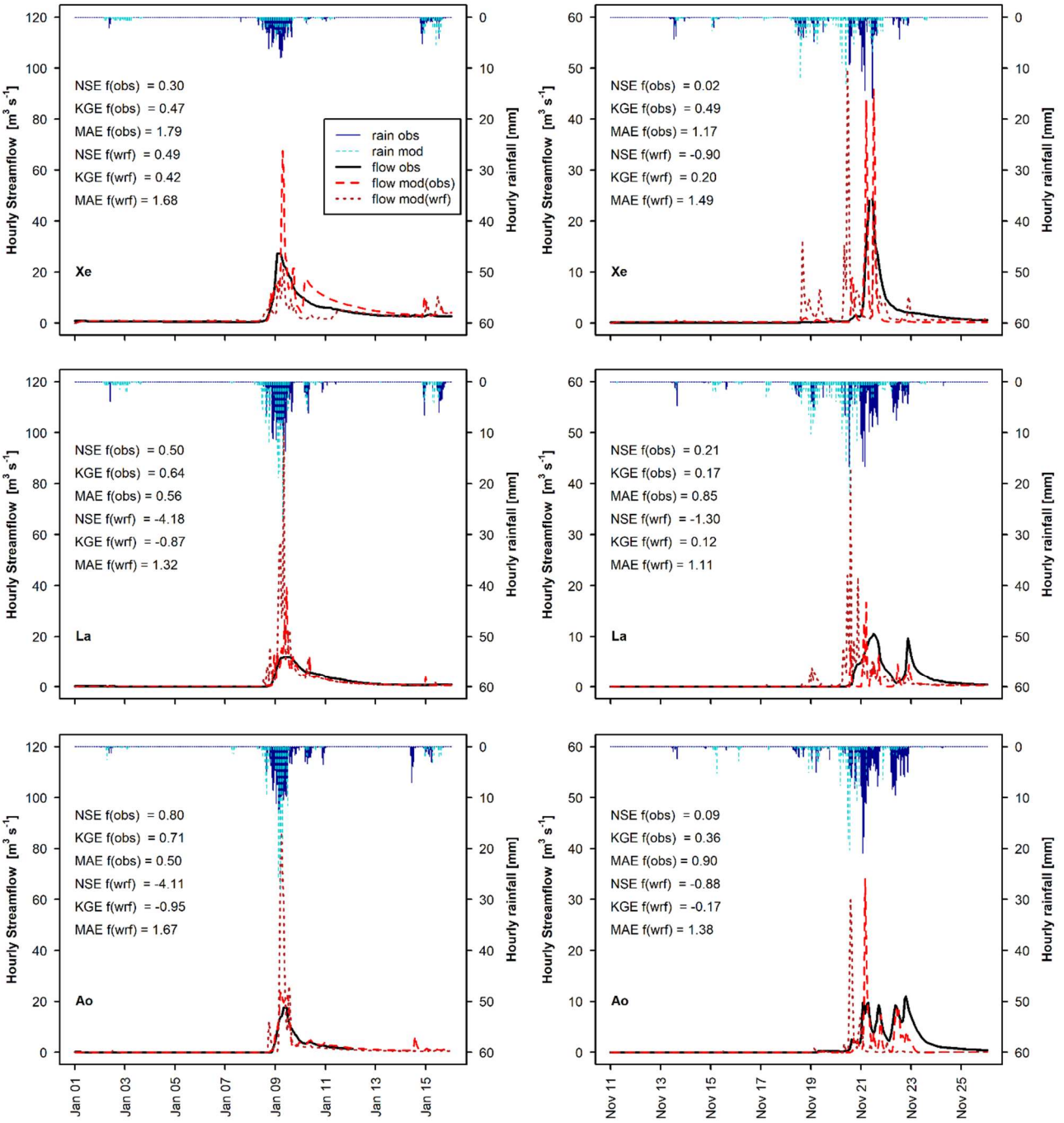

Figure 10. Observed hourly hydrographs (flow obs) and hydrographs obtained with the calibrated WRF-Hydro model (flow mod) forced with observed rainfall (rain obs) and with WRF-modelled rainfall (rain wrf) for both Jan 1989 (left) and Nov 1994 (right), for three watersheds (see Table 1 for watershed short names); modelled flow performance indices (NSE, Nash-Sutcliffe Efficiency; KGE, Kling-Gupta Efficiency; BIAS) are shown as well.

6 Conclusion

This study evaluates streamflow simulations of the one-way coupled atmospheric-hydrologic model WRF-Hydro, forced with observed and WRF-modeled rainfall, during two extreme events, over 22 small mountain watersheds in Cyprus (area below 100 km^2). Following model calibration and validation with observed rain, the model was run with WRF-downscaled (1 × 1 km^2) re-analysis precipitation data (ERA-Interim). These forcing data represent best-performing hindcasts of two extreme rainfall events, i.e. a model product that is as similar as possible to reality and considered sub-optimal.

Overall, the selected four calibration parameters (REFKDT, Soil depth, the baseflow bucket exponent, and the maximum baseflow bucket capacity) were sufficient to obtain good model performance during model calibration in these steeply sloping and geologically complex watersheds. Sensitivity analysis showed that REFKDT can be calibrated beyond the

suggested 0.5-5.0 range, having an effect on infiltration till a value of approximately 100.0. A Soil depth of 1.0 m, representative of the thin soils characterizing the study area, rather than the default value of 2.0 m, resulted in an average increase in *NSE* values of 0.14. Modifications of deep drainage coefficients and MODIS soil types based on geology reduced the peak flow overestimation by up to 40% in watersheds characterized by a fractured and very permeable bedrock. The overland roughness routing factor reduced the streamflow but showed a very limited effect on delaying flow. A straightforward calibration of the baseflow reservoir based on low flow fitting (exponent) and reservoir filling time (maximum capacity) was a good mean for obtaining a reasonable simulation of the hydrograph recession in most watersheds. Calculated daily *NSE* values were higher than 0.5 in 16 out of the 22 modeled watersheds in Jan 1989 (calibration) and in eight watersheds in Nov 1994 (validation). Negative *NSE* values were found in ~~the smallest watershed (5.2 km^2), caused by high relative errors for small differences; and in five~~ three watersheds located at high elevation where an underestimation of the snow fraction, computed by the LSM, ~~with a high fraction of permeable bedrock, where drainage from the bottom of the soil column~~ may have occurred ~~faster than was simulated~~. Modelled snow height, and possible improvements deriving from the use of alternatives routines (e.g. Noah MP), should be checked with observed snow depth data, which were not available for this study.

The comparison of modelled and observed hourly streamflow showed that almost all peak flows were overestimated by the calibrated model. Modelled hourly streamflow fit the Jan 1989 hydrographs relatively well, but much less so the Nov 1994 discharges. This performance loss in Nov 1994 was due to a pulse-like behavior of the modeled streamflow related to an immediate response to rainfall, which could be attenuated by higher channel roughness coefficients.

Streamflow obtained with WRF-modelled rainfall forcing showed high discrepancies with observations, despite the good agreement between modelled and observed precipitation (average *NSE* of 0.83 and 0.49 for Jan 1989 and Nov 1994, respectively). This suggests that model calibration with modelled rainfall forcing is not optimal for small mountain watersheds and should be carefully evaluated if no other options are available. As a consequence, ~~therefore~~ WRF rainfall forecasts may not be sufficiently accurate for predicting the location and size of ~~the~~ specific floods of such small mountain watersheds. However, due to the relatively small errors in total precipitation (average relative difference over the 22 watersheds of 17% and for 20% Jan 1989 and Nov-1994 events, respectively) and simulated daily maxima (average relative difference over the 22 watersheds of 22% and 18% for Jan 1989 and Nov-1994 events, respectively), modelled rainfall data could be suitable for investigating the effect of climate change on extreme rainfall and flood events. From the results presented and discussed, it emerges that future studies could focus on various aspects of the modelling system to improve the simulation results of both precipitation and streamflow. Soil properties could be specifically calibrated for the study area. For a continuous, long-term streamflow analysis, an evaluation of the sensitivity of the baseflow reservoir parameters could be carried out. Also, ~~T~~the model could be improved by incorporating an option for time-dependent roughness coefficients to represent vegetation growth in ephemeral and intermittent streams in semi-arid environments. A model configuration with variable soil depths could also improve model performance, especially in mountain environments.

7 Acknowledgments

This research was funded by the BINGO project (Bringing INnovation to onGOing water management), European Union's Horizon 2020 Research and Innovation programme, under the Grant Agreement number 641739. For computation, this work was supported by the Cy-Tera Project (NEA ΥΠΟΔΟΜΗ/ΣΤΡΑΤΗ/0308/31), which is co-funded by the European Regional Development Fund and the Republic of Cyprus through the Research Promotion Foundation. Authors would also like to thank the Water Development Department of Cyprus for data sharing and support.

Code/Data availability

WRF-Hydro is an open-source community model. The code and additional information can be found at https://ral.ucar.edu/projects/wrf_hydro/overview. WRF-Hydro simulated streamflow at the watershed outlets, for the two events (Jan 1989 and Nov 1994) and the two forcing (observed and modelled precipitation) are available on https://zenodo.org (DOI: 10.5281/zenodo.3952420).

Author contribution

Conceptualization, C.C., A.B., G.Z.; methodology, C.C., A.B; software, C.C., G.Z., I.S.; formal analysis, C.C.; investigation, C.C., I.S.; data curation, C.C., G.Z., I.S.; writing—original draft preparation, C.C.; writing—review and editing, A.B., G.Z, I.S., J.A.; supervision, A.B., J.A.; funding acquisition, A.B.

Competing interests

The authors declare no competing interests.

References

Arnault, J., Wagner, S., Rummler, T., Fersch, B., Bliefernicht, J., Andresen, S. and Kunstmann, H.: Role of Runoff–Infiltration Partitioning and Resolved Overland Flow on Land–Atmosphere Feedbacks: A Case Study with the WRF-Hydro Coupled Modeling System for West Africa, J. Hydrometeorol., 17(5), 1489–1516, doi:10.1175/JHM-D-15-0089.1, 2016.

Arnault, J., Wei, J., Rummler, T., Fersch, B., Zhang, Z., Jung, G., Wagner, S. and Kunstmann, H.: A joint soil-vegetation-atmospheric water tagging procedure with WRF-Hydro: Implementation and application to the case of precipitation partitioning in the upper Danube river basin, Water Resour. Res., 55(7), 6217–6243, doi:10.1029/2019WR024780, 2019.

Avolio, E., Cavalcanti, O., Furnari, L., Senatore, A. and Mendicino, G.: Brief communication: Preliminary hydro-meteorological analysis of the flash flood of 20 August 2018 in Raganello Gorge, southern Italy, Nat. Hazards Earth Syst. Sci., 19(8), 1619–1627, doi:https://doi.org/10.5194/nhess-19-1619-2019, 2019.

Brunke, M. A., Broxton, P., Pelletier, J., Gochis, D., Hazenberg, P., Lawrence, D. M., Leung, L. R., Niu, G.-Y., Troch, P. A. and Zeng, X.: Implementing and Evaluating Variable Soil Thickness in the Community Land Model, Version 4.5 (CLM4.5), J. Clim., 29(9), 3441–3461, doi:10.1175/JCLI-D-15-0307.1, 2016.

Camera, C., Zomeni, Z., Noller, J. S., Zissimos, A. M., Christoforou, I. C. and Bruggeman, A.: A high resolution map of soil types and physical properties for Cyprus: A digital soil mapping optimization, Geoderma, 285, 35–49, doi:10.1016/j.geoderma.2016.09.019, 2017.

Camera, C., Djuma, H., Bruggeman, A., Zoumides, C., Eliades, M., Charalambous, K., Abate, D. and Faka, M.: Quantifying the effectiveness of mountain terraces on soil erosion protection with sediment traps and dry-stone wall laser scans, CATENA, 171, 251–264, doi:10.1016/j.catena.2018.07.017, 2018.

Christofi, C., Bruggeman, A., Kuells, C. and Constantinou, C.: Hydrochemical evolution of groundwater in gabbro of the Troodos Fractured Aquifer. A comprehensive approach, Appl. Geochem., 114, 104524, doi:10.1016/j.apgeochem.2020.104524, 2020.

Cleintaur, M. R., Knox, G. J. and Ealey, P. J.: The geology of Cyprus and its place in the eastern Mediterranean framework, Geol. En Mijnb., 56(1), 66–82, 1977.

Constantinidou, K., Zittis, G. and Hadjinicolaou, P.: Variations in the Simulation of Climate Change Impact Indices due to Different Land Surface Schemes over the Mediterranean, Middle East and Northern Africa, Atmosphere, 10(1), 26, doi:10.3390/atmos10010026, 2019.

Cyprus Geological Survey Department: Geological map of Cyprus (1:250,000), [online] Available from: http://www.moa.gov.cy/moa/gsd/gsd.nsf/page32_en/page32_en?OpenDocument (Accessed 28 January 2020), 1995.

Di Luzio, M., Johnson, G. L., Daly, C., Eischeid, J. K. and Arnold, J. G.: Constructing Retrospective Gridded Daily Precipitation and Temperature Datasets for the Conterminous United States, J. Appl. Meteorol. Climatol., 47(2), 475–497, doi:10.1175/2007JAMC1356.1, 2008.

Djuma, H., Bruggeman, A., Zissimos, A., Christoforou, I., Eliades, M. and Zoumides, C.: The effect of agricultural abandonment and mountain terrace degradation on soil organic carbon in a Mediterranean landscape, CATENA, 195, 104741, doi:10.1016/j.catena.2020.104741, 2020.

Ek, M. B., Mitchell, K. E., Lin, Y., Rogers, E., Grunmann, P., Koren, V., Gayno, G. and Tarpley, J. D.: Implementation of Noah land surface model advances in the National Centers for Environmental Prediction operational mesoscale Eta model, J. Geophys. Res. Atmospheres, 108(D22), doi:10.1029/2002JD003296, 2003.

Fersch, B., Senatore, A., Adler, B., Arnault, J., Mauder, M., Schneider, K., Völksch, I. and Kunstmann, H.: High-resolution fully-coupled atmospheric–hydrological modeling: a cross-compartment regional water and energy cycle evaluation, Hydrol. Earth Syst. Sci. Discuss., 1–37, doi:https://doi.org/10.5194/hess-2019-478, 2019.

Givati, A., Gochis, D., Rummler, T. and Kunstmann, H.: Comparing one-way and two-way coupled hydrometeorological forecasting systems for flood forecasting in the Mediterranean region, Hydrology, 3(2), 19, doi:10.3390/hydrology3020019, 2016.

Gochis, D. J., Yu, W. and Yates, D. N.: WRF-Hydro Technical Description and User's Guide, version 3.0, NCAR Tech. Doc., 123 pages, 2015.

Julien, P. Y., Saghafian, B. and Ogden, F. L.: Raster-Based Hydrologic Modeling of Spatially-Varied Surface Runoff1, JAWRA J. Am. Water Resour. Assoc., 31(3), 523–536, doi:10.1111/j.1752-1688.1995.tb04039.x, 1995.

Kling, H., Fuchs, M. and Paulin, M.: Runoff conditions in the upper Danube basin under an ensemble of climate change scenarios, J. Hydrol., 424–425, 264–277, doi:10.1016/j.jhydrol.2012.01.011, 2012.

Krause, P., Boyle, D. P. and Bäse, F.: Comparison of different efficiency criteria for hydrological model assessment, in Advances in Geosciences, vol. 5, pp. 89–97, Copernicus GmbH., 2005.

Lahmers, T. M., Gupta, H., Castro, C. L., Gochis, D. J., Yates, D., Dugger, A., Goodrich, D. and Hazenberg, P.: Enhancing the Structure of the WRF-Hydro Hydrologic Model for Semiarid Environments, J. Hydrometeorol., 20(4), 691–714, doi:10.1175/JHM-D-18-0064.1, 2019.

Le Coz, M., Bruggeman, A., Camera, C. and Lange, M. A.: Impact of precipitation variability on the performance of a rainfall–runoff model in Mediterranean mountain catchments, Hydrol. Sci. J., 61(3), 507–518, doi:10.1080/02626667.2015.1051983, 2016.

Legates, D. R. and McCabe, G. J.: Evaluating the use of "goodness-of-fit" Measures in hydrologic and hydroclimatic model validation, Water Resour. Res., 35(1), 233–241, doi:10.1029/1998WR900018, 1999.

Lin, T.-S. and Cheng, F.-Y.: Impact of soil moisture initialization and soil texture on simulated land–atmosphere interaction in Taiwan, J. Hydrometeorol., 17(5), 1337–1355, doi:10.1175/JHM-D-15-0024.1, 2016.

Maidment, D. R.: Conceptual Framework for the National Flood Interoperability Experiment, JAWRA J. Am. Water Resour. Assoc., 53(2), 245–257, doi:10.1111/1752-1688.12474, 2017.

Naabil, E., Lamptey, B. L., Arnault, J., Olufayo, A. and Kunstmann, H.: Water resources management using the WRF-Hydro modelling system: Case-study of the Tono dam in West Africa, J. Hydrol. Reg. Stud., 12, 196–209, doi:10.1016/j.ejrh.2017.05.010, 2017.

Nash, J. E. and Sutcliffe, J. V.: River flow forecasting through conceptual models part I — A discussion of principles, J. Hydrol., 10(3), 282–290, doi:10.1016/0022-1694(70)90255-6, 1970.

Ning, L., Zhan, C., Luo, Y., Wang, Y. and Liu, L.: A review of fully coupled atmosphere-hydrology simulations, J. Geogr. Sci., 29(3), 465–479, doi:10.1007/s11442-019-1610-5, 2019.

Niu, G.-Y., Yang, Z.-L., Mitchell, K. E., Chen, F., Ek, M. B., Barlage, M., Kumar, A., Manning, K., Niyogi, D., Rosero, E., Tewari, M. and Xia, Y.: The community Noah land surface model with multiparameterization options (Noah-MP): 1. Model description and evaluation with local-scale measurements, J. Geophys. Res. Atmospheres, 116(D12), doi:10.1029/2010JD015139, 2011.

Reyers, M., Feldmann, H., Mieruch, S., Pinto, J. G., Uhlig, M., Ahrens, B., Früh, B., Modali, K., Laube, N., Moemken, J., Müller, W., Schädler, G. and Kottmeier, C.: Development and prospects of the regional MiKlip decadal prediction system over Europe: predictive skill, added value of regionalization, and ensemble size dependency, Earth Syst. Dyn., 10(1), 171–187, doi:https://doi.org/10.5194/esd-10-171-2019, 2019.

Richards, L. A.: Capillary conduction of liquids through porous mediums, Physics, 1(5), 318–333, doi:10.1063/1.1745010, 1931.

Rummler, T., Arnault, J., Gochis, D. and Kunstmann, H.: Role of lateral terrestrial water flow on the regional water cycle in a complex terrain region: investigation with a fully coupled model system, J. Geophys. Res. Atmospheres, 124(2), 507–529, 2019.

Rutledge, A. T.: Computer Programs for Describing the Recession of Ground-Water Discharge and for Estimating Mean Ground-Water Recharge and Discharge from Streamflow Records--Update, [online] Available from: https://water.usgs.gov/ogw/part/ (Accessed 28 January 2020), 1988.

Saha, S., Moorthi, S., Wu, X., Wang, J., Nadiga, S., Tripp, P., Behringer, D., Hou, Y.-T., Chuang, H., Iredell, M., Ek, M., Meng, J., Yang, R., Mendez, M. P., van den Dool, H., Zhang, Q., Wang, W., Chen, M. and Becker, E.: The NCEP Climate Forecast System Version 2, J. Clim., 27(6), 2185–2208, doi:10.1175/JCLI-D-12-00823.1, 2014.

Schaake, J. C., Koren, V. I., Duan, Q.-Y., Mitchell, K. and Chen, F.: Simple water balance model for estimating runoff at different spatial and temporal scales, J. Geophys. Res. Atmospheres, 101(D3), 7461–7475, doi:10.1029/95JD02892, 1996.

Senatore, A., Mendicino, G., Gochis, D. J., Yu, W., Yates, D. N. and Kunstmann, H.: Fully coupled atmosphere-hydrology simulations for the central M editerranean: Impact of enhanced hydrological parameterization for short and long time scales, J. Adv. Model. Earth Syst., 7(4), 1693–1715, doi:10.1002/ 2015MS000510, 2015.

Silver, M., Karnieli, A., Ginat, H., Meiri, E. and Fredj, E.: An innovative method for determining hydrological calibration parameters for the WRF-Hydro model in arid regions, Environ. Model. Softw., 91, 47–69, doi:10.1016/j.envsoft.2017.01.010, 2017.

Skamarock, W. C. and Klemp, J. B.: A time-split nonhydrostatic atmospheric model for weather research and forecasting applications, J. Comput. Phys., 227(7), 3465–3485, doi:10.1016/j.jcp.2007.01.037, 2008.

Verri, G., Pinardi, N., Gochis, D., Tribbia, J., Navarra, A., Coppini, G. and Vukicevic, T.: A meteo-hydrological modelling system for the reconstruction of river runoff: the case of the Ofanto river catchment, Nat. Hazards Earth Syst. Sci., 17(10), 1741, doi:10.5194/nhess-17-1741-2017, 2017.

Water Development Department: Dams of Cyprus, Ministry of Agriculture, Natural Resources and Environment, Nicosia, Cyprus., 2009.

Wehbe, Y., Temimi, M., Weston, M., Chaouch, N., Branch, O., Schwitalla, T., Wulfmeyer, V., Zhan, X., Liu, J. and Mandous, A. A.: Analysis of an extreme weather event in a hyper-arid region using WRF-Hydro coupling, station, and satellite data, Nat. Hazards Earth Syst. Sci., 19(6), 1129–1149, doi:10.5194/nhess-19-1129-2019, 2019.

Wigmosta, M. S. and Lettenmaier, D. P.: A comparison of simplified methods for routing topographically driven subsurface flow, Water Resour. Res., 35(1), 255–264, doi:10.1029/1998WR900017, 1999.

Wigmosta, M. S., Vail, L. W. and Lettenmaier, D. P.: A distributed hydrology-vegetation model for complex terrain, Water Resour. Res., 30(6), 1665–1679, doi:10.1029/94WR00436, 1994.

Yucel, I., Onen, A., Yilmaz, K. K. and Gochis, D. J.: Calibration and evaluation of a flood forecasting system: Utility of numerical weather prediction model, data assimilation and satellite-based rainfall, J. Hydrol., 523, 49–66, doi:10.1016/j.jhydrol.2015.01.042, 2015.

Zhang, Z., Arnault, J., Wagner, S., Laux, P. and Kunstmann, H.: Impact of Lateral Terrestrial Water Flow on Land-Atmosphere Interactions in the Heihe River Basin in China: Fully Coupled Modeling and Precipitation Recycling Analysis, J. Geophys. Res. Atmospheres, 124(15), 8401–8423, doi:10.1029/2018JD030174, 2019.

Zittis, G., Hadjinicolaou, P. and Lelieveld, J.: Role of soil moisture in the amplification of climate warming in the eastern Mediterranean and the Middle East, Clim. Res., 59(1), 27–37, doi:10.3354/cr01205, 2014.

Zittis, G., Bruggeman, A., Camera, C., Hadjinicolaou, P. and Lelieveld, J.: The added value of convection permitting simulations of extreme precipitation events over the eastern Mediterranean, Atmospheric Res., 191, 20–33, doi:10.1016/j.atmosres.2017.03.002, 2017.